

2 AUG 1972

Report 3577

NAVAL SHIP RESEARCH AND DEVELOPMENT CENTER

Bethesda, Md. 20034



AD 746120

OPTICAL PHASE AND INTENSITY FLUCTUATIONS IN A REFRACTIVE INDEX MICROSTRUCTURE

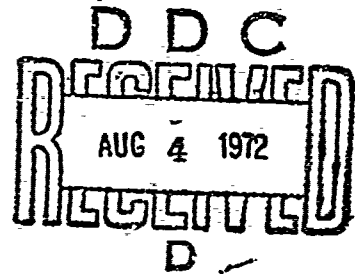
A Mathematical Analysis

by

Alan S. Fields

Optical Phase and Intensity Fluctuations in a
Refractive Index Microstructure - A Mathematical Analysis

Approved for public release;
distribution unlimited.



PROPULSION AND AUXILIARY SYSTEMS DEPARTMENT
Annapolis

RESEARCH AND DEVELOPMENT REPORT

Reproduced by
NATIONAL TECHNICAL
INFORMATION SERVICE
U S Department of Commerce
Springfield VA 22151

July 1972

Report 3577

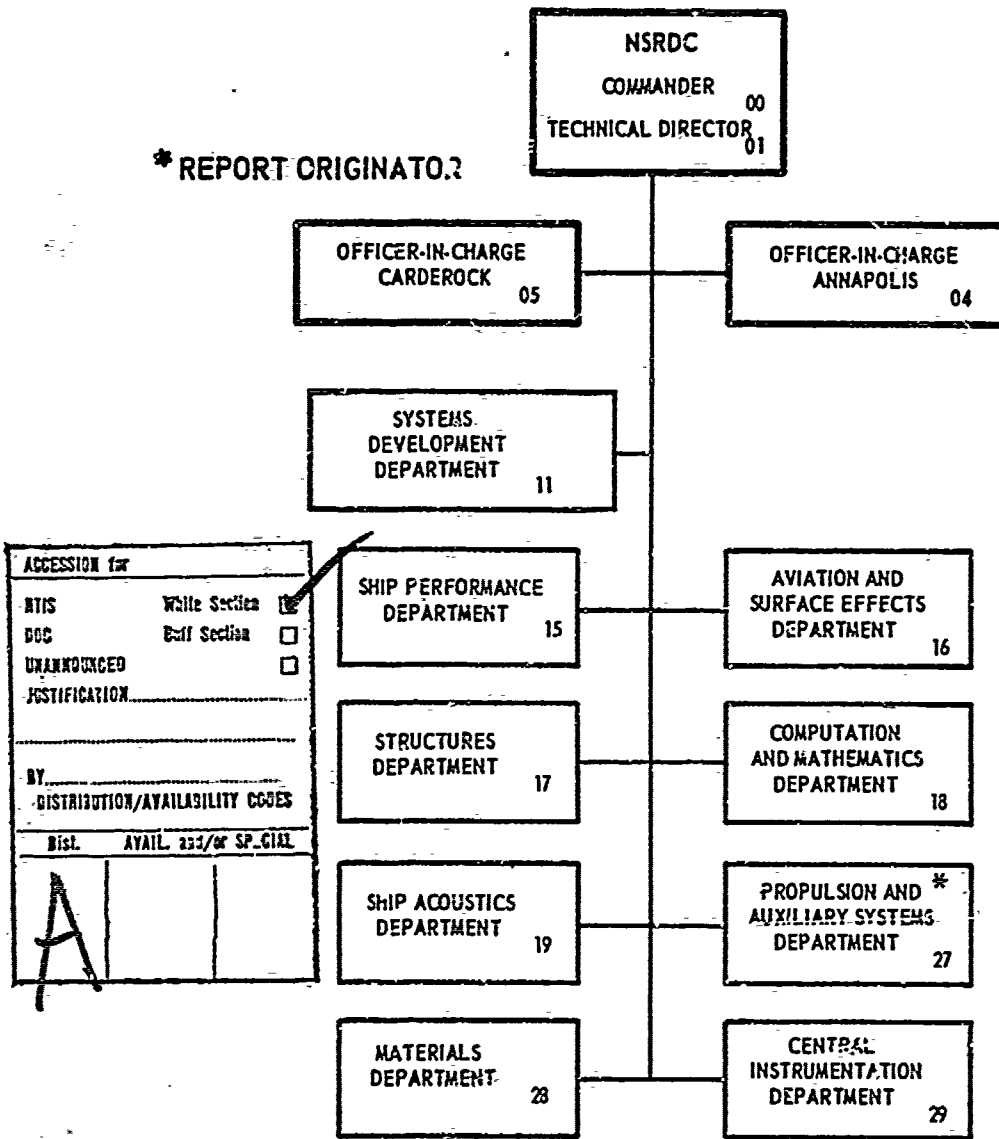
61

The Naval Ship Research and Development Center is a U. S. Navy center for laboratory effort directed at achieving improved sea and air vehicles. It was formed in March 1967 by merging the David Taylor Model Basin at Carderock, Maryland with the Marine Engineering Laboratory at Annapolis, Maryland.

Naval Ship Research and Development Center
Bethesda, Md. 20034

MAJOR NSRDC ORGANIZATIONAL COMPONENTS

* REPORT ORIGINATOR



ACCESSION for	
NTIS	White Section <input checked="" type="checkbox"/>
DOC	Buff Section <input type="checkbox"/>
UNANNOUNCED	<input type="checkbox"/>
JUSTIFICATION	
BY	
DISTRIBUTION/AVAILABILITY CODES	
DISL	AVAIL. 233/SP_GIAL
A	

Security Classification

UNCLASSIFIED

DOCUMENT CONTROL DATA - R & D

(Security classification of title, body of abstract and indexing annotation must be entered when the overall report is classified)

1. ORIGINATING ACTIVITY (Corporate author) Naval Ship Research and Development Center Annapolis Laboratory Annapolis, Maryland 21402		2a. REPORT SECURITY CLASSIFICATION Unclassified	
		2b. GROUP	
3. REPORT TITLE Optical Phase and Intensity Fluctuations in a Refractive Index Microstructure			
4. DESCRIPTIVE NOTES (Type of report and inclusive dates) A Mathematical Analysis			
5. AUTHOR(S) (First name, middle initial, last name) Alan S. Fields			
6. REPORT DATE July 1972		7a. TOTAL NO. OF PAGES 65	7b. NO. OF REFS 9
8a. CONTRACT OR GRANT NO. b. PROJECT NO. Task Area Z-R001-01-01 c. Task 0401 d. Work Unit 1-623-158		8a. ORIGINATOR'S REPORT NUMBER(S) 3577 8b. OTHER REPORT NO(S) (Any other numbers that may be assigned this report) 6-196	
10. DISTRIBUTION STATEMENT Approved for public release; distribution unlimited.			
11. SUPPLEMENTARY NOTES		12. SPONSORING MILITARY ACTIVITY NAVSHIPS (SHIPS 031)	
13. ABSTRACT Studies have been published which extend and apply the Kolomogorov theory of turbulence to the fluctuations of optical refractive index in the ocean due to salinity and temperature microstructure. Mathematical models of some of the statistical properties of these fluctuations are developed to provide continuous functions obeying the various Fourier transform relationships provided by the studies. The continuous functions are utilized to characterize the phase and intensity fluctuations of a plane, monochromatic optical wave passes through such a turbulent medium. The knowledge of the relationship between fluctuations of the optical parameters and the refractive index microstructure provides a basis for the utilization of laser beams as data links or in studies of the propagating medium. (Author)			

DD FORM 1473 (PAGE 1)
1 NOV 65

S/N 0101-807-6801

ja

UNCLASSIFIED
Security Classification

14. KEY WORDS	LINK A		LINK B		LINK C	
	ROLE	WT	ROLE	WT	ROLE	WT
Spectra Waves Equations Light sources Refractive index Microstructure Intensity Fluctuations Perturbations Mathematical model						

DEPARTMENT OF THE NAVY
NAVAL SHIP RESEARCH AND DEVELOPMENT CENTER
BETHESDA, MD. 2034

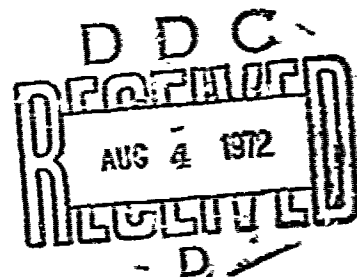
OPTICAL PHASE AND INTENSITY FLUCTUATIONS
IN A REFRACTIVE INDEX MICROSTRUCTURE

A MATHEMATICAL ANALYSIS

by
Alan S. Fields



Approved for public release;
distribution unlimited.



July 1972

6-196

Report 3577

ABSTRACT

Studies have been published which extend and apply the Kolomogorov theory of turbulence to the fluctuations of optical refractive index in the ocean due to salinity and temperature microstructure.

Mathematical models of some of the statistical properties of these fluctuations are developed to provide continuous functions obeying the various Fourier transform relationships provided by the studies. The continuous functions are utilized to charecterize the phase and intensity fluctuations of a plane, monochromatic optical wave passed through such a turbulent medium.

The knowledge of the relationship between fluctuations of the optical parameters and the refractive index microstructure provides a basis for the utilization of laser beams as data links or in studies of the propagating medium.

ADMINISTRATIVE INFORMATION

This report is part of the Naval Ship Research and Development Center's FR/IED Program, Task Area Z-R001-01-01, Task 0401, Work Unit 1-623-158.

ACKNOWLEDGMENT

This work could not have been accomplished without the expertise and encouragement of the Project Engineer, Mr. Donald R. Laster, and the efforts of Mr. E. M. Stanley. In addition, the computer program developed by Dr. Feodor Theilheimer and Mr. Robert Wybraniec provided the major results.

TABLE OF CONTENTS

	<u>Page</u>
ABSTRACT	iii
ADMINISTRATIVE INFORMATION	iv
ACKNOWLEDGMENT	iv
LIST OF SYMBOLS	vii
INTRODUCTION	1
OPTICAL INTENSITY AND PHASE FLUCTUATIONS	1
Descriptions of the Intensity and Phase Fluctuations Based on the Solution of the Wave Equation by Spectral Expansion	1
Assumptions Required for the Solution of the Wave Equation by Spectral Expansion	2
MATHEMATICAL MODELING OF THE REFRACTIVE INDEX	
MICROSTRUCTURE IN THE OCEAN	4
Spectral Information	4
Structure Function Information	6
Selection of a Model	7
OPTICAL PROPAGATION PROPERTIES BASED ON THE MODEL	13
DISCUSSION	14
CONCLUSIONS	17
TECHNICAL REFERENCES	18
LIST OF FIGURES	
Figure 1 - Curve; One-Dimensional Spectrum of Refractive Index Variations, $E_{nl}(k)$, as a Function of Wave Number, k	
Figure 2 - Curve; Three-Dimensional Spectrum of Refractive Index Variations, $E_{nn}(k)$, as a Function of Wave Number, k	
Figure 3 - Curve; Modified Three-Dimensional Spectrum of Refractive Index Variations, $E_n(k)$, as a Function of Wave Number, k	
Figure 4 - Curve; Structure Function of Refractive Index Variations, $D_{nl}(r)$, as a Function of Distance, r	
Figure 5 - Curve; Computed Phase Structure Function for Temperature, $D_{\phi T}(\rho)$, as a Function of Separation Distance, ρ , and Distance Traversed, L	
Figure 6 - Curve; Computed Phase Structure Function for Salinity, $D_{\phi S}(\rho)$, as a Function of Separation Distance, ρ , and Distance Traversed, L	
Figure 7 - Curve; Computed Logarithmic Amplitude Structure Function for Temperature, $D_{\ln T}(\rho)$, as a Function of Separation Distance, ρ , and Distance Tra- versed, L	
Figure 8 - Curve; Computed Logarithmic Amplitude Structure Function for Salinity, $D_{\ln S}(\rho)$, as a Function of Separation Distance, ρ , and Distance Traversed, L	
Figure 9 - Curve; Length Normalized Optical Phase Variance, ϕ^2/L , as a Function of Distance Traversed, L	

TABLE OF CONTENTS (Cont)

- Figure 10 - Curve; Optical Intensity Variance, $\overline{X_1^2}$, as a
Function of Distance Traversed, L
Figure 11 - Curve; Optical Phase Structure Function, D_ϕ ,
at Separation Distance $\rho = 0.2 \times 10^{-4}$ as a
Function of Distance Traversed, L

APPENDIXES

- Appendix A - Statistical Descriptions of Random Functions
and Random Fields (18 pages)
Appendix B - Computer Program for Calculating the Optical
Propagation Properties (7 pages)

INITIAL DISTRIBUTION

LIST OF SYMBOLS

Symbol	Definition	Units
ϵ	Kinematic energy dissipation rate	$\text{cm}^2/\text{sec}^{3*}$
θ_0	Angular aperture	radians
ν	Kinematic viscosity	cm^2/sec
$\bar{\phi}_2$	Optical phase variance	- -
ρ	Cylindrical (two-dimensional) distance	cm
λ	Light source wavelength	cm
κ	Light source wave number	cm^{-1}
l_0	Smallest geometrical dimension of inhomogeneities	cm
ψ	Logarithm of optical wave ¹ complex amplitude	- -
ω	Radian frequency	radians/sec
τ	Time	sec
∇	Gradient operator	- -
$\Gamma(\cdot)$	Gamma function	- -
$B(\cdot)$	Correlation function	- -

*Abbreviations used in this text are from the GPO Style Manual, 1967, unless otherwise noted.

¹Subscript 0 indicates unperturbed component.

Subscript 1 indicates perturbed component.

No subscript indicates sum of perturbed and unperturbed (following the notation of Tatarski).

²Subscript l refers to logarithmic-amplitude variations.

Subscript ϕ refers to phase variations.

Subscript n refers to refractive index variations.

Subscript α refers to a general phenomenon.

Single subscript indicates modified three-dimensional.

Single subscript with 1 indicates one-dimensional.

Single subscript with 2 indicates two-dimensional.

Double subscript indicates three-dimensional.

B_1	Universal constant	--
$Ci(\cdot)$	Cosine integral function	--
D	Molecular diffusion coefficient ³	cm^2/sec
$D(\cdot)$	Structure function ²	--
$E(\cdot)$	Spectral function ²	--
$J_0(\cdot)$	Bessel function of zero order	--
k	Wave number	cm^{-1}
k_s	Inertial viscous intercept	cm^{-1}
$k(1), k(3)$	Asymptote intercept in one- and three-dimensional spectra, respectively	cm^{-1}
$\log(\cdot)$	Logarithm function, base 10	--
k_1	Arbitrarily selected start of inertial region	cm^{-1}
k_3	Start of viscous region (wave number)	cm^{-1}
k_5	Start of decay region (wave number) ³	cm^{-1}
k'_5	Cutoff of decay region for integration	cm^{-1}
k_ρ	Two-dimensioned wave number	cm^{-1}
$K_2(\cdot)$	Modified Bessel function of second kind of order 2	--
n	Refractive index ¹	--
L	Length of patch in medium	cm
c^*	Universal constant	--
S_1	Phase of perturbed wave function	--
X_1	Logarithmic amplitude of perturbed wave function	--
u	Optical wave function ¹	--
$\omega(\cdot)$	Spectrum	--

³Subscript T for temperature.
Subscript S for salinity.

INTRODUCTION

Considerable effort has been applied to descriptions of the temperature and salinity microstructure of the ocean. These descriptions, both theoretically and empirically derived, are not yet definitive. There is, however, limited agreement between theory and measurement. The results have been summarized and discussed by Stanley.¹ The descriptions are based on the Fourier transform related structure function (with distance as the argument) and spectrum (with wave number as the argument). These descriptions are composed of separate functions, applicable in specific ranges of the arguments.

For a similar characterization on a measurement plane of the optical intensity and phase fluctuations of a plane, monochromatic wave which has been passed a given distance through the turbulent ocean, the descriptions of the refractive index microstructure of the ocean (based on the temperature and salinity microstructure) must be mathematically smooth to eliminate unreal effects caused by "corners" in the descriptions. That is, a smooth transition function must be found between the descriptions in the separate ranges.

Expressions valid over the entire range of interest are developed to describe the refractive index fluctuations. These expressions are shown as to agree with present theory and available data. The desired descriptions of the optical fluctuations are found. As some of the statistical descriptions are not in the common literature, the analysis techniques for obtaining these descriptions are reviewed in appendix A for both scalar quantities and vector fields.

OPTICAL INTENSITY AND PHASE FLUCTUATIONS

The optical intensity and phase fluctuations of a plane, monochromatic wave passed through a turbulent medium, characterized by refractive index microstructure, will be described on a measurement plane. The measurement plane is perpendicular to the original direction of the wave and situated such that the wave passes a distance L through the medium. The wave number of the (light) source is κ , the wave length is λ . The medium is described by the three-dimensional spectrum of its refractive index microstructure, $E_{nn}(k_0)$.

DESCRIPTIONS OF THE INTENSITY AND PHASE FLUCTUATIONS BASED ON THE SOLUTION OF THE WAVE EQUATION BY SPECTRAL EXPANSION

The fluctuations of an optical wave can be described by amplitude and phase fluctuations. By taking the logarithm, one

¹Superscripts refer to similarly numbered entries in the Technical References at the end of the text.

separates the fluctuations into the sum of the logarithmic amplitude or intensity and phase fluctuations, which can then be treated separately if the fluctuations are small. Tatarski,² chapter 7, applies the methods of "small" and "smooth" perturbations to the solution of the wave equation by spectral expansion to obtain the desired statistical descriptions in terms of the refractive index spectrum.

The two-dimensional spectra in the measurement plane of the logarithmic intensity $E_{\ell 2}(k_\rho)$, and phase, $E_{\phi 2}(k_\rho)$, are given as

$$E_{\ell 2}(k_\rho) = \pi \kappa^2 L \left(1 - \frac{k}{k_\rho^2} \sin \frac{k_\rho^2 L}{k} \right) E_{nn}(k_\rho) \quad (1)$$

$$E_{\phi 2}(k_\rho) = \pi \kappa^2 L \left(1 + \frac{k}{k_\rho^2} \sin \frac{k_\rho^2 L}{k} \right) E_{nn}(k_\rho). \quad (2)$$

The corresponding correlation functions are

$$B_{\ell 2}(\rho) = 2\pi \int_0^\infty J_0(k_\rho \rho) E_{\ell 2}(k_\rho) k_\rho dk_\rho \quad (3)$$

$$B_{\phi 2}(\rho) = 2\pi \int_0^\infty J_0(k_\rho \rho) E_{\phi 2}(k_\rho) k_\rho dk_\rho \quad (4)$$

The corresponding structure functions are

$$D_{\ell 2}(\rho) = 4\pi \int_0^\infty \left[1 - J_0(k_\rho \rho) \right] E_{\ell 2}(k_\rho) k_\rho dk_\rho \quad (5)$$

$$D_{\phi 2}(\rho) = 4\pi \int_0^\infty \left[1 - J_0(k_\rho \rho) \right] E_{\phi 2}(k_\rho) k_\rho dk_\rho \quad (6)$$

Appendix A reviews these statistical descriptions.

ASSUMPTIONS REQUIRED FOR THE SOLUTION OF THE WAVE EQUATION BY SPECTRAL EXPANSION

As stated, Tatarski,² chapter 7, applies the methods of "small" and "smooth" perturbations to the solution of the wave

equation by spectral expansion. These methods require less restrictive assumptions than those required if the principles of geometric optics are employed (Tatarski,² chapter 6).

Tatarski considers a medium for which the mean refractive index is unity. More general results are required here, but the substitution is simple and does not affect the resulting relationships. The derivation of the relationships involves extensive work. As the effort here merely makes use of the results, only a brief description of some of the assumptions will be given to indicate the range of physical validity of the results. The models are evaluated beyond the range of physical validity only to demonstrate the characteristics of the functions. The assumptions are:

- The wavelength of the light source is much smaller than the smallest Euclidian dimension of the inhomogeneities in the spatial distribution of refractive index, ℓ_0 .

$$\lambda \ll \ell_0. \quad (7)$$

- The fluctuations in refractive index, n_1 , are much smaller than the mean refractive index, n_0 , where the refractive index, $n = n_0 + n_1$.

$$n_1 \ll n_0. \quad (8)$$

- The wave is expressed as the sum of a perturbed component, u_1 , and an unperturbed component, u_0 , where the perturbed component is much smaller than the unperturbed one. More precisely, the assumption is

$$|u_1/u_0| \lesssim |n_1/n_0| \ll 1. \quad (9)$$

Let $\log(u_0) = \psi_0$, $u_1/u_0 = \psi_1$, and $\log(u) = \psi$. Provided that $|u_1/u_0| \ll 1$, then $\psi_1 = \psi - \psi_0$. As $|n_1/n| \ll 1$, $|\nabla\psi| \ll |\nabla\psi_0|$ is required. As $|\nabla\psi_0| 2k = 2\pi/\lambda$, it is required that $\lambda|\nabla\psi_1| \ll 2\pi$. Writing $\psi_1 = X_1 + iS_1$, it can be shown that $|X_1| < |S_1|$, so the conditions here are satisfied if the phase variations, S_1 , satisfy

$$|\nabla S_1| \ll 2\pi/\lambda. \quad (10)$$

Under these conditions, "the angle of scattering of the waves by refractive index inhomogeneities is of order no greater than $\theta_0 = \lambda/\ell_0$ and is thus small. Therefore, the value of ψ_1 can

only be appreciably affected by the inhomogeneities included in a cone with vertex at the observation point, with axis directed towards the wave source, and with angular aperture $\theta_0 = \lambda/l_0 \ll 1$."2

MATHEMATICAL MODELING OF THE REFRACTIVE INDEX MICROSTRUCTURE IN THE OCEAN

In order to permit computer aided calculation based on equations (1) through (6), and to prevent excessive errors due to artificial sharp corners in E_{nn} , a smooth, continuous function is sought as the mathematical model. The difficulty is that the available theoretical and empirical information concerns itself with the inertial, viscous-convective, and decay regions of turbulence and turbulent mixing separately. Thus, there are descriptions of the refractive index variations in each of these regions but there is no definitive information as to the manner in which the phenomena behave in the transitions between regions. The criterion of selection for the mathematical model of the spectrum is that it and its Fourier transform, the correlation function, agrees with the available information in the known regions. Once this is assured, the model can be applied to describing the optical fluctuations.

On the bases of work by Tatarski² and Laster,³ Stanley¹ shows that the descriptions of refractive index fluctuations (correlation, structure, or spectral functions) are a linear combination of those of temperature and salinity fluctuations. These functions and the coefficients of the linear combination are scaled by temperature, salinity, and mean refractive index, as given by Laster.³ They will be discussed here in an unscaled, separated form.

SPECTRAL INFORMATION

Table 1 gives the form of the spectrum in the three regions.

TABLE 1
SPECTRA FORMS

Region	One-Dimensional	Three-Dimensional
Inertial	$\frac{1}{2}B_1 \epsilon^{-1/3} k^{-5/3}$	$\frac{1}{4} \cdot \frac{5}{3} B_1 \pi^{-1} \epsilon^{-1/3} k^{-11/3}$
Viscous-Convective	$\frac{1}{2}q^* \nu^{1/2} \epsilon^{-1/2} k^{-1}$	$\frac{1}{4}q^* \pi^{-1} \nu^{1/2} \epsilon^{-1/2} k^{-3}$
Decay	$\frac{1}{2}q^* \nu^{1/2} \epsilon^{-1/2} k^{-1} \cdot \exp(-D^{3/2} k^2 q^* / \epsilon^{1/2})$	$\frac{1}{4}q^* \pi^{-1} \nu^{1/2} \epsilon^{-1/2} k^{-3} \cdot \exp(-D^{3/2} k^2 q^* / \epsilon^{1/2})$

In the inertial region, the one-dimensional spectrum is taken from Gibson and Schwartz⁴ except for the factor 1/2 which is employed so that the one-dimensional spectrum is defined over negative and positive wave numbers, instead of just positive. The three-dimensional spectrum is defined based on equation (11) from Tatarski.²

$$E_{\alpha\alpha}(k) = - \frac{1}{2\pi k} \frac{\partial E_{\alpha 1}(k)}{\partial k} . \quad (11)$$

This is in agreement with Stanley,¹ as his modified three-dimension spectrum, has a factor $B_2 = \frac{5}{3}B_1$ which corresponds to the results of equation (12) from Hinze.⁵

$$E_{\alpha}(k) = 4\pi k^2 E_{\alpha\alpha}(k) . \quad (12)$$

B_1 is a universal constant given by Gibson and Schwartz⁴ as 0.31. The factor 5/3 is apparent from equation (11).

A similar transformation is employed in the viscous-convective region. The factor q^* , given as approximately 2.0 by Stanley¹, is given by Grant, et al,⁶ as nominally twice that (3.7 ± 1.5). The difference is apparently due to the difference in definition of the spectra.

The spectral representations in the decay region only approximately follow equation (11). The form of the three-dimensional term is found in Stanley¹ and is the only available representation.

Batchelor⁷ predicts that the inertial subrange asymptote and the viscous subrange asymptote (the relations of table 1) intersect at

$$k = k_s = \left(\frac{\epsilon}{\nu} \right)^{1/4} . \quad (13)$$

The intersection calculated for one-dimensional spectra gives

$$k^{(1)} = \left(\frac{B_1}{q^*} \right)^{3/2} \left(\frac{\epsilon}{\nu^3} \right)^{1/4} = \left(\frac{B_1}{q^*} \right)^{3/2} k_s . \quad (14)$$

The intersection calculated for three-dimensional spectra gives

$$k^{(3)} = \left(\frac{5}{3}\right)^{3/2} \left(\frac{B_1}{q^*}\right)^{3/2} \left(\frac{\epsilon}{\nu^3}\right)^{1/4} = 2.15k_s. \quad (15)$$

This difference has occurred in the literature. Grant, et al,⁶ note a factor of $(2.4 \pm 0.8) \times 10^{-2} k_s$ working with a one-dimensional spectrum, while Nye and Brodkey⁸ noted a value $5.0 \times 10^{-2} k_s$ working with the three-dimensional spectrum.

For the mathematical model, it is convenient to normalize the one-dimensional spectra by the factor

$$q^* \nu^{1/2} \epsilon^{-1/2} / 4\pi, \quad (16)$$

making the one-dimensional spectrum in the viscous-convective region simply

$$2\pi k^{-1}. \quad (17)$$

The result for the inertial region is

$$2\pi (B_1/q^*) k_s^{2/3} k^{-5/3}. \quad (18)$$

STRUCTURE FUNCTION INFORMATION

The structure function information is taken from Batchelor⁷ and appears in table 2. Of course, the structure function rises to a constant beyond the inertial region. In the inertial region, relationship, a proportionality constant is needed which Batchelor⁷ assumes is unity.

TABLE 2
STRUCTURE FUNCTION FORMS

Region	Function
Decay	$\left(\frac{q^*}{2}\right) \left(\frac{1}{6D}\right) r^2$
Viscous-Convective	$\left(\frac{q^*}{2}\right) \left(\frac{\nu}{\epsilon}\right)^{1/2} \ln\left(\frac{\epsilon r^4}{4\nu D^2}\right)$
Inertial	$\left(\frac{q^*}{2}\right) \epsilon^{-1/3} r^{2/3}$

SELECTION OF A MODEL

Representative values of the known parameters are as follows:

$$\epsilon = 10^{-3} \text{ kinetic energy dissipation rate}^1$$

$$\nu = 10^{-2} \text{ kinematic viscosity}^3$$

$$B_1 = 0.31 \text{ universal constant.}^4$$

This gives $k_S = 5.623$ from equation (13). Selecting $q^* = 3.815$, $k^{(1)} = 0.023k_S$ from equation (14) and $k^{(3)} = 0.049k_S$ from equation (15). Let

$$k_3 = k^{(3)} = 0.28;$$

therefore

$$k^{(1)} = k_3/2.15.$$

Let

$$k_5 = \left(\frac{\epsilon}{\nu D^2} \right)^{1/4},$$

where for representative values³ for temperature $D = D_T = 10^{-3}$ ($k_{5T} = 18$) and for salinity, $D = D_S = 10^{-5}$ ($k_{5S} = 180$).

Equation (18), for the inertial region, may now be written as

$$2\pi(3/5)k_3^{2/3}k^{-5/3}, \quad (19)$$

and the viscous-convective decay regions may be combined as equation (20).

$$2\pi k^{-1} \exp \left[-2(k/k_5)^2 \right]. \quad (20)$$

Equation (18) for the inertial region and equation (20) for the viscous-convective and decay regions, when considered in their respective ranges, provide the same information as table 1; that

is, a one-dimensional spectrum varying as $k^{-5/3}$ until $k_3/2.15$, then as k^{-1} until approximately k_5 , then an exponential decay. The viscous-convective and decay regions are combined as k_3 is small compared to k_5 .

Permitting the spectrum to vary as $k^{-5/3}$ all the way back to $k = 0$ is equivalent to assuming an infinite energy source, which is not physically realizable. Instead, equation (19) will be said to hold only for k larger than k_1 , where k_1 is much smaller than k_3 . This provides for what is essentially a scaling of the problem. The selection of a value for k_1 sets the variance (the value of the correlation function at zero argument) and the upper constant of the structure function (the value at infinite argument which is twice the variance). For k less than k_1 , the spectrum is a constant.

The forms of the spectral and structure functions are summarized in table 3. The structure functions are normalized by equation (16) as were the spectra.

TABLE 3
SUMMARY OF STRUCTURE AND SPECTRAL FUNCTION FORMS

Wave Number Range	Spectrum	Structure Function	Distance Range
$k < k_1$	Constant	Constant	$r > 1/k_1$
$k_1 < k < k_3$	$2^{-1} (3/5) k_3^{2/3} k^{-5/3}$	$2^{-1} (12.3) (3/5) (k_3 r)^{2/3}$	$1/k_3 < r < 1/k_1$
$k_3 < k < k_5$	$2^{-1} k^{-1}$	$2^{-1} \ln(k_5^2 r^2 / k_3^2)$	$1/k_5 < r < 1/k_3$
$k > k_5$	$2^{-1} k^{-1} \exp[-2(k/k_5)^2]$	$2^{-1} (1/6) (k_5 r)^2$	$r < 1/k_5$

Equation (21) is a smooth function which satisfies table 3 for the spectrum.

$$2^{-1} \left[\frac{(3/5) k_3^{2/3}}{(k^2 + k_1^2)^{5/6}} + \frac{1}{(k^2 + k_3^2)^{1/2}} \right] \exp -2(k/k_5)^2 \quad (21)$$

Tatarski² gives the following Fourier transform pair and related information.

$$B(\tau) = \int_{-\infty}^{\infty} \cos(\omega\tau) f(\omega) d\omega \quad (22)$$

$$B(\tau) = \frac{2\pi\sqrt{\pi}}{2^{a-1}\Gamma(a+1/2)} \int_{-\infty}^{\infty} \cos(\omega\tau) \omega^{2a} d\omega \quad (23)$$

$$B(0) = \frac{2\pi\sqrt{\pi}}{\Gamma(a+1/2)} \quad (24)$$

$$B(\infty) = 0 \quad (25)$$

$$W(\omega) = 2\pi \frac{\omega_0^{2a}}{(\omega^2 + \omega_0^2)^{a+1/2}} \quad (26)$$

$$D(\tau) = \frac{4\pi\sqrt{\pi}}{\Gamma(a+1/2)} \left[\Gamma(a) - \frac{(\omega_0\tau)^a}{2^{a-1}} K_a(\omega_0\tau) \right] \quad (27)$$

$$D(\infty) = 2B(0) = \frac{4\pi\sqrt{\pi}}{(a+1/2)} \quad (28)$$

$$D(\tau) = \frac{4\pi\sqrt{\pi}}{\Gamma(a+1/2)} \frac{1}{2a} \frac{\Gamma(a-1)(\omega_0\tau)^{2a}}{2^{a-1}} ; \omega_0\tau < 1, \quad |a| < 1 \quad (29)$$

where B is a correlation function, D is the associated structure function, and W is the associated spectrum. As the first term in the bracket in equation (21) becomes negligibly small before the exponential multiplier departs significantly from unity, the exponential can be neglected. Writing this term as

$$\frac{3}{5} \left(\frac{k_3}{k_1} \right)^{2/3} \frac{k_1^{2/3}}{(k^2 + k_1^2)^{5/6}} \quad (30)$$

and considering equation (26) with $\omega_0 = k_1$, $a = 1/3$, $\omega = k$, we can see that the corresponding structure function can be derived

from equation (27). At small values of the argument, equation (29) is valid, and the structure function is

$$\left(\frac{3}{5}\right)\left(\frac{k_3}{k_1}\right)^{2/3} \frac{4\sqrt{\pi}}{\Gamma(5/6)} \left[\frac{1}{2/3} \frac{\Gamma(2/3) (k_1 r)^{2/3}}{2^{-1/3}} \right]$$

$$= 2\pi(48.25)(3/5)(k_3 r)^{2/3}; \quad r < 1/k_3. \quad (31)$$

By performing an approximate integration for the second term in equation (21), including the multiplicative exponential, one gets

$$8\pi \left[1 + \ln k_5' - \ln k_3 - \frac{\sin k_3 r}{k_3 r} + \text{Ci}(k_3 r) - \text{Ci}(k_5' r) \right]$$

$$- 8\pi \sum_{n=1}^{\infty} \left[\frac{(-1)^{n+1} (k_3 r)^{2n}}{(2n+1)!} + \frac{(-1)^n r^{2n} (k_3^{2n} - k_5'^{2n})}{2n(2n)!} \right]$$

$$\begin{cases} 2\pi (k_5' r)^2 & ; \quad r < 1/k_5 \\ 8\pi [0.577 + \ln(k_5' r)] & ; \quad 1/k_5 < r < 1/k_3 \\ 8\pi [1 + \ln(k_5'/k_3)] & ; \quad r > 1/k_3 \end{cases} \quad (32)$$

where

$$\text{Ci}(z) = - \int_z^{\infty} \frac{\cos t}{t} dt = \gamma + \ln z + \sum_{n=1}^{\infty} \frac{(-1)^n z^{2n}}{2n(2n)!}$$

is the cosine integral function and $\gamma = 0.577$ is Euler's constant.⁹

The factor k_5' is the wave number in the neighborhood of k_5 at which the exponential decay can be considered to begin to strongly affect the function for the purposes of the approximate integration. If k_5' is selected so that in the range $r < 1/k_5$, the result in equation (32) matches the desired results in table 3, then

$$(k_5^i/k_5) = \sqrt{1/6} = 0.408. \quad (33)$$

This is a reasonable selection for k_5^i , as the exponential multiplier in the spectrum evaluated at k_5^i is 0.72, and it decreases rapidly thereafter.

The desired result for $r < 1/k_5$ no longer exists when the results in equations (31) and (32) are added for $r \leq 1/k_3$. In order to eliminate these undesired effects of the $r^{2/3}$ dependence, the spectrum model is changed to

$$2\pi \left[\frac{(3/5)k_3^{2/3}}{(k^2 + k_3^2)^{5/6}} - \frac{(3/5)k_3^{2/3}}{(k^2 + k_3^2)^{5/6}} + \frac{1}{(k^2 + k_3^2)^{1/2}} \right] \cdot \exp \left[-2(k/k_5)^2 \right]. \quad (34)$$

In finding the structure function associated with the first two terms of equation (34), the exponential can be neglected. The result is

$$\begin{aligned} & \left(\frac{3}{5} \right) \frac{4\pi\sqrt{\pi}}{\Gamma(2/3)} \left\{ \Gamma(1/3) \left[(k_3/k_1)^{2/3} - 1 \right] - \right. \\ & \left. 2^{2/3} \left[(k_3/k_1)^{2/3} (k_1 r)^{1/3} K_{1/3}(k_1 r) - (k_3 r)^{1/3} K_{1/3}(k_3 r) \right] \right\} \\ = & \begin{cases} 0 & ; r < 1/k_3 \\ 2\pi (21.55) (3/5) (k_3 r)^{2/3} - 31.74 & ; 1/k_3 < r < 1/k_1 \\ 31.74 \left[(k_3/k_1)^{2/3} - 1 \right] & ; r > 1/k_1 \end{cases} \quad (35) \end{aligned}$$

Combining this with the result obtained from the last term of equation (34) as given by equation (32), we get,

$$D_{nl}(r) = \begin{cases} 31.74 \left[(k_3/k_1)^{2/3} - 1 \right]; & r > 1/k_1 \\ 2\pi \left[-0.33 + \ln(k_5/k_3) + (21.55)(3/5)(k_3 r)^{2/3} \right] & 1/k_3 < r < 1/k_5 \\ 2\pi \left[0.108 + \ln(k_5^4 r^4 / 4) \right]; & 1/k_5 < r < 1/k_3 \\ 2\pi (1/6) (k_5 r)^2 & r < 1/k_5 \end{cases} \quad (36)$$

Comparing the results in equation (36) to the information on table 3 we see:

- The constant result for $r > 1/k_1$.

- The desired two-thirds dependence for $1/k_3 < r < 1/k_1$. This term is multiplied by approximately 1.75; but as stated above table 2, a proportionality constant of unity was assumed, so that 1.75 is not unreasonable.

- The desired logarithmic term for $1/k_5 < r < 1/k_3$ with a negligible additive constant.

- The desired square law dependence for $r < 1/k_5$.

Thus, the selected model for the one-dimensional spectrum in equation (34) meets the specified criterion that its structure function agree with existing data. Note also that the intercepts of the asymptotes of the model are still as stated in equations (14) and (15). As shown in table 1, the three-dimensional model does not exactly correspond to the one-dimensional model. In the model given below, an error term exists which can be seen to be a multiplicative factor on each term consisting of unity plus a constant on the order of unity times the factor $(k/k_5)^2$. The factor has a negligibly small effect except in the decay region. The exponential for the decay region is heuristically chosen in the references to cut off what would be an infinite power contribution from the k^{-1} dependence. In this light, considering that the error term times the exponential falls off as rapidly as the exponential itself in the decay region, the approximation error is negligible.

The selected model is given in equations (37) through (39) and displayed graphically in figures 1 through 4.

$$E_{nl}(k) = 2\pi \left[\frac{(3/5)k_3^{2/3}}{(k^2 + k_1^2)^{5/6}} - \frac{(3/5)k_3^{2/3}}{(k^2 + k_2^2)^{5/6}} + \frac{1}{(k^2 + k_3^2)^{1/2}} \right] \cdot \exp \left[-2(k/k_5)^2 \right] \quad (37)$$

$$E_{nn}(k) = \left[\frac{k_3^{2/3}}{(k^2 + k_1^2)^{11/6}} - \frac{k_3^{2/3}}{(k^2 + k_3^2)^{11/6}} + \frac{1}{(k^2 + k_3^2)^{3/2}} \right] \cdot \exp \left[-2(k/k_5)^2 \right] \quad (38)$$

$$D_{r,1}(r) = 31.74 \left[(k_3/k_1)^{2/3} - 1 \right] - 50.38 \left[(k_3/k_1)^{2/3} (k_1 r)^{1/3} K_{1/3}(k_1 r) - (k_3 r)^{1/3} K_{1/3}(k_3 r) \right] + 25.13 \left[1 + \ln(k_3/k_5) - \frac{\text{Si}(k_3 r)}{k_3 r} + \text{Ci}(k_3 r) - \text{Ci}(k_5 r) \right] \quad (39)$$

where

$$\begin{aligned} k_1 &= 0.001 \text{ (selected)} \\ k_3 &= 0.28 \\ k_{5T} &= 18 \\ k_{5S} &= 180 \\ k_5^* &= 0.408 k_S. \end{aligned}$$

OPTICAL PROPAGATION PROPERTIES BASED ON THE MODEL

Using the model given by equation (38), the two-dimensional spectra of the logarithmic amplitude and phase fluctuations are obtained by equations (1) and (2). The associated structure functions for temperature and salinity can be obtained from the inte-

grals given in equations (5) and (6). A computer program was prepared by Dr. F. Theilheimer and Mr. R. Wybraniec of the Computation and Mathematics Department, Bethesda, to perform these integrations by means of the eight-point Gauss quadrature formula. A sample program listing and additional information are given in appendix B.

Each integral is calculated with unequal intervals starting at 0 and ending at the first interval past 1000. The intervals are of increasing length because the greatest degree of fluctuation occurs for the small limits of integration.

Figures 5 and 6 display the structure functions of the phase variations for temperature and salinity, respectively. Figures 7 and 8 display the structure functions of the logarithmic amplitude variations for temperature and salinity, respectively. Figure 9 displays the variance of the phase variations for both temperature and salinity. Figure 10 displays a similar result for the logarithmic amplitude variations.

DISCUSSION

The mathematical model, equations (37) through (39), is shown to be consistent with the structure and spectral function information based on the referenced analytical and experimental results. The functional form of the model is such that computer aided computation of the optical propagation properties is possible. The smoothness of these computer results partially demonstrates the suitability of the model and the computational technique.

The primary results are given in figures 5 through 10. These are the results of the integrals given by equations (5) and (6). These integrals are two-dimensional Fourier transforms. For purposes of discussion, the term integrand will refer to the two-dimensional spectra given in equations (1) and (2), each multiplied by the variable of integration k_{ρ} . The functions

$$1 \pm \frac{\kappa}{k_{\rho}^2 L} \sin \frac{k_{\rho}^2 L}{\kappa} \quad (40)$$

will be referred to as the "window." The results

$$1 \pm \frac{\kappa}{k_{\rho}^2 L} \sin \frac{k_{\rho}^2 L}{\kappa} = \begin{cases} 1 \pm \left[1 - \left(\frac{k_{\rho}^2 L}{\kappa} \right)^2 \right]; & \frac{k_{\rho}^2 L}{\kappa} < 0.1 \\ 1 & ; \frac{k_{\rho}^2 L}{\kappa} > 10 \end{cases} \quad (41)$$

will be utilized. Thus the window for the logarithmic amplitude variations is

$$\left[\frac{k_{\rho}^2 L}{\kappa} \right]^2 ; \frac{k_{\rho}^2 L}{\kappa} < 0.1$$

$$= ; \frac{k_{\rho}^2 L}{\kappa} > 10$$
(42)

while, for phase variations, the window is

$$2 ; \frac{k_{\rho}^2 L}{\kappa} < 0.1$$

$$1 ; \frac{k_{\rho}^2 L}{\kappa} > 10.$$
(43)

As the three-dimensional spectrum has an insignificant contribution to the integrals for $k < k_1$, the window does not affect the integrals if

$$\frac{k_1^2 L}{\kappa} > 10$$
(44)

$$L > \frac{10\kappa}{k_1^2} = 1.32 \times 10^{12}.$$
(45)

The term "L is large" or "large L" shall refer to $L > 1.32 \times 10^{12}$. When L is large, as the window does not have effect, L linearly scales the results, but has no effect on the shape of the structure function. The factor

$$1 - J_0(k_{\rho} \rho)$$
(46)

shall be referred to as the transformation function, and the result

$$1 - J_0(k_\rho \rho) = \begin{cases} 0; & k_\rho \rho < 0.1 \\ 1; & k_\rho \rho > 10 \end{cases} \quad (47)$$

will be employed.

The results will be discussed first in terms of the functional relationship to the separation distance in the measurement plane, ρ , then as a function of L , the distance traversed through the medium.

When L is large, the integrand contributes no significant "energy" (or, to paraphrase Batchelor,⁷ no temperature or salinity stuff) for $k < k_1$, thus, the structure function should stop increasing for $\rho < 1/k_1 = 10^3$, as the results show (see the $\ell = 10^{13}$ curves for this portion of the discussion). As ρ is decreased, the transformation function inhibits the contribution of the integrand to wave numbers on the order of $1/\rho$ and above. At k_5 the integrand decays on its own. As ρ decreases from $1/k_1$ to $1/k_3$ (the inertial range), the results show a $\rho^{3/2}$ dependence. For $\rho < 1/k_5$, the decay range, a ρ^2 dependence is seen. Tatarski² predicts the ρ^2 dependence in the decay range but finds $\rho^{5/3}$ in the inertial range. His result is based on approximate analytical integration techniques that are not experimentally confirmed. No further discussion is possible, based on existing information, except to state that his results can be duplicated by the computer techniques utilized here, and by analytical techniques, assuming, as he did, the inertial range spectrum asymptote ($k_0^{-11/3}$) exists for all k_0 , rather than utilizing the given model.

In the viscous-convective range, $1/k_5 < \rho < 1/k_3$, the results show a rise, that is, the curve is above the inertial and decay asymptotes. As this exists in a range of ρ in which physical measurements can be made, the phenomenon is significant. As Tatarski² worked with a medium with no viscous-convective range, he had no such results. Similarly, as his spectrum rises to infinity as k approaches zero, his results show no flattening in the structure function. The flattening represents the finite "energy" driving the turbulence. If a smaller value of k_1 was selected, say at the scale size of the ocean, it is apparent that the variance would be larger. The curves are easily extended for any k_1 less than the selected 1000 reciprocal centimeters, and it is clear that the selected value of k_1 was small enough not to affect the results, that is, to permit extrapolation.

The L dependence of the shape of the phase structure function is slight. The shape of the curves is not a function of L , while the amplitude is linearly dependent upon L . Figure 9 shows that at L of the order of 10^{11} , the coefficient of the linear dependence

of the variance on L and ρ 's. This is noted in figures 5 and 6 also. At large ρ , a separation change between curves occurs at large L . As ρ is decreased, the separation change between curves moves to smaller L . This is simply explained by the window for the phase variation. For large L , the value of k_0 at which the window decreases is on the order of k_1 , the location of the peak of $k_0 E_{nn}(k_0)$. As L is decreased, the window affects the function at larger values of k_0 ; therefore, the effect occurs at smaller values of ρ . Once the window decrease occurs for $k_0 > k_5$, the effect is lost. Figure 11 further illustrates this by showing the structure function at small ρ as a function of L . It is significant that the change occurs at physically meaningful values of L .

The L dependence of the shape of the logarithmic amplitude structure functions is stronger as the logarithmic amplitude window has a stronger L dependence. As L is decreased, increasingly more of the lower wave number (longer length) portion of the spectrum is eliminated or "cut off" by the window. This is apparent as long wavelength phenomena cannot affect short distance measurements, but will appear as nonstationarities in the mean and be eliminated in a structure function measurement (see appendix A). Thus, as L is increased, the lowest wave number at which the integrand provides "energy" is increased. Hence, the separation distance, ρ , at which the structure function flattens is decreased (see figures 7 and 8). As the "cutoff" of the window is given approximately as \sqrt{L}/κ , the "cutoff" value of ρ for $1/k_5 < \rho < 1/k_1$ is $\sqrt{\kappa/L}$. For $L > 10\kappa/k_1^2$, the window no longer changes the integrand. Similarly, for $L < .1\kappa/k_5^2$, the spectrum itself "cuts off," so the window no longer has an effect other than scaling.

Figure 10 shows the dependence of the variance on L . For $L > \kappa/k_1^2$, L is seen to linearly scale the variance. For $\kappa/k_3^2 < L < \kappa/k_1^2$, as Tatarski² predicts, the variance varies as $L^{11/6}$. For $L < \kappa/k_5^2$, the variance changes as L^3 . Once again, a rise corresponding to the viscous-convective range is evident. For $\kappa/k_5^2 < L < \kappa/k_3^2$, the variance is above the $L^{11/6}$ and L^3 asymptotes. This is significant, as in physically meaningful ranges of L , from 1 centimeter to 100 meters, the variance of the salinity variations, for example, is above the asymptotes by a factor of 10.

CONCLUSIONS

• In sea water, the existence of the viscous-convective subrange in the temperature and salinity (hence refractive index) spectra causes a significant increase in the fluctuations of the phase and logarithmic amplitude of the optical wave. The increased optical fluctuations caused by the salinity microstructure occur for optical path lengths of about 1 centimeter to 1000 meters; thus experimental confirmation is feasible.

• The use of structure functions instead of correlation functions to characterize the spatial fluctuations is considered a more meaningful approach because the physical phenomena being described are at best only quasi-stationary, with stationary first increments assumed. The structure function approach directly provides the functional dependences, particularly at small distances, because these dependences are not hidden by the variance as they would be in the case of correlation functions.

• The smooth, mathematical representation developed for the refractive index spectra satisfies theoretical and experimental data where available and is suitable for computer solution of the integral equations. Further, this spectra representation is sufficiently general so that it can be used for various media by appropriate selection of the spectral cutoff and breakpoint wave numbers.

TECHNICAL REFERENCES

- 1 - Stanley, E. M., "Temperature, Salinity and Optical Refractive Index Microstructure in the Ocean," NAVSHIPRANDLAB Annapolis R&D Rept 3063 (Jan 1970)
- 2 - Tatarski, V. I., Wave Propagation in a Turbulent Medium, R. A. Silverman (Translation), New York, McGraw-Hill Book Co. (1964)
- 3 - Laster, D. R., "Proposed Optical Methods for Measuring Ocean Micro-Scale Turbulence Effects," Marine Sciences Instrumentation, Vol. 4, New York, Plenus Press (1968)
- 4 - Gibson, C. H., and W. H. Schwartz, "The Universal Equilibrium Spectra of Turbulent Velocity and Scalar Fields," J. Fluid Mech., Vol. 10, pp. 365-385 (1963)
- 5 - Hinze, J. O., Turbulence, New York, McGraw-Hill Book Co. (1959)
- 6 - Grant, H. L., et al, "The Spectrum of Turbulent Fluctuations in Turbulent Flow," J. Fluid Mech., Vol. 34, pp. 423-442 (1968)
- 7 - Batchelor, G. K., "Small-Scale Variation of Converted Quantities Like Temperature in Turbulent Fluid," J. Fluid Mech., Vol. 5, pp. 113-133 (1959)
- 8 - Nye, J. O., and R. S. Bradkey, "The Scalar Spectrum in the Viscous Convective Subrange," J. Fluid Mech., Vol. 29, pp. 151-163 (1967)
- 9 - Abramowitz, M., and T. A. Stegun (Editors), Handbook of Mathematical Functions, National Bureau of Standards, U. S. Dept. of Commerce, Applied Math., Series 55, Washington, D.C., pp. 230-233 (1964)

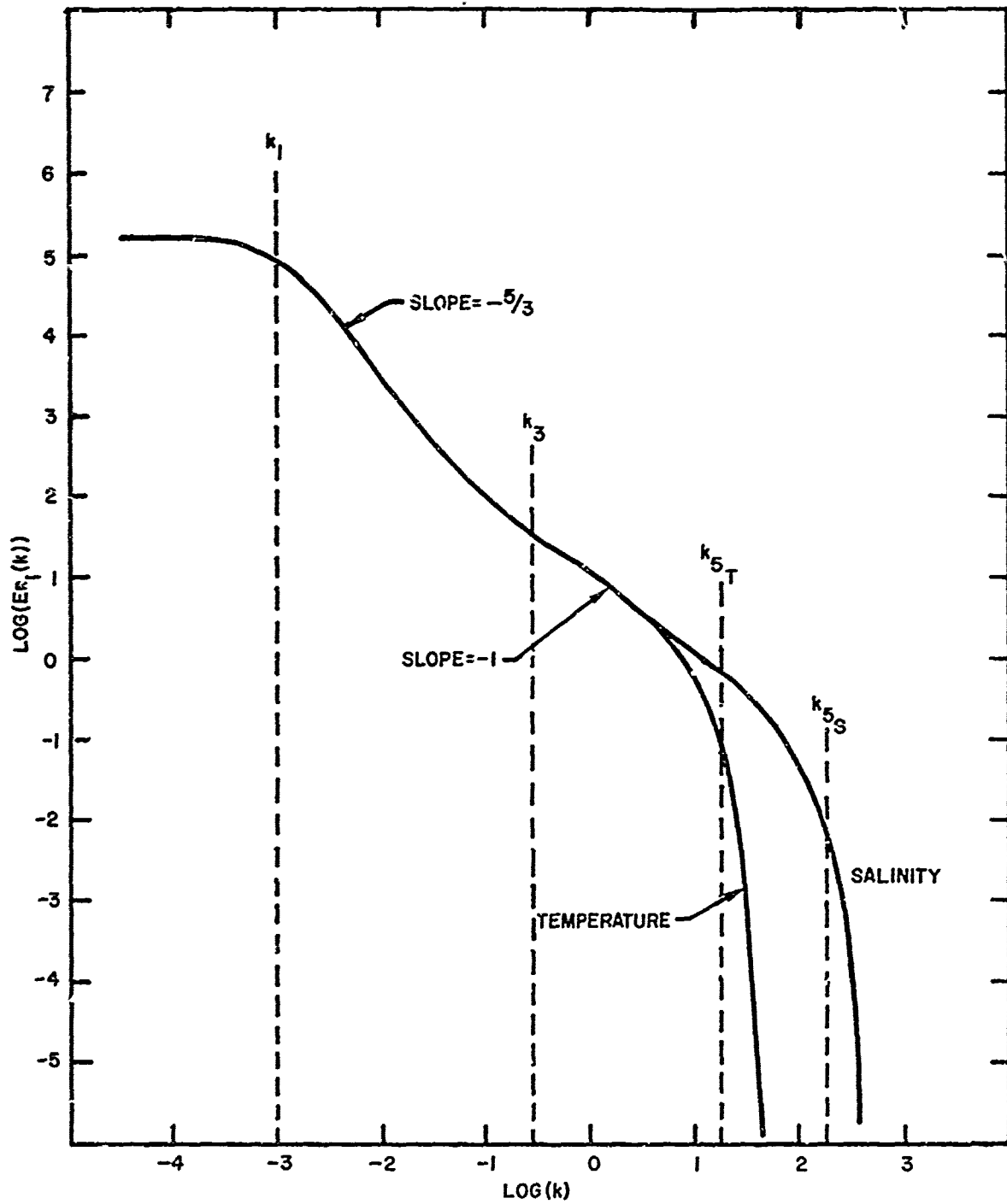


Figure 1
 One-Dimensional Spectra of Refractive Index
 Variations, $E_{n1}(k)$, as a Function of Wave Number, k

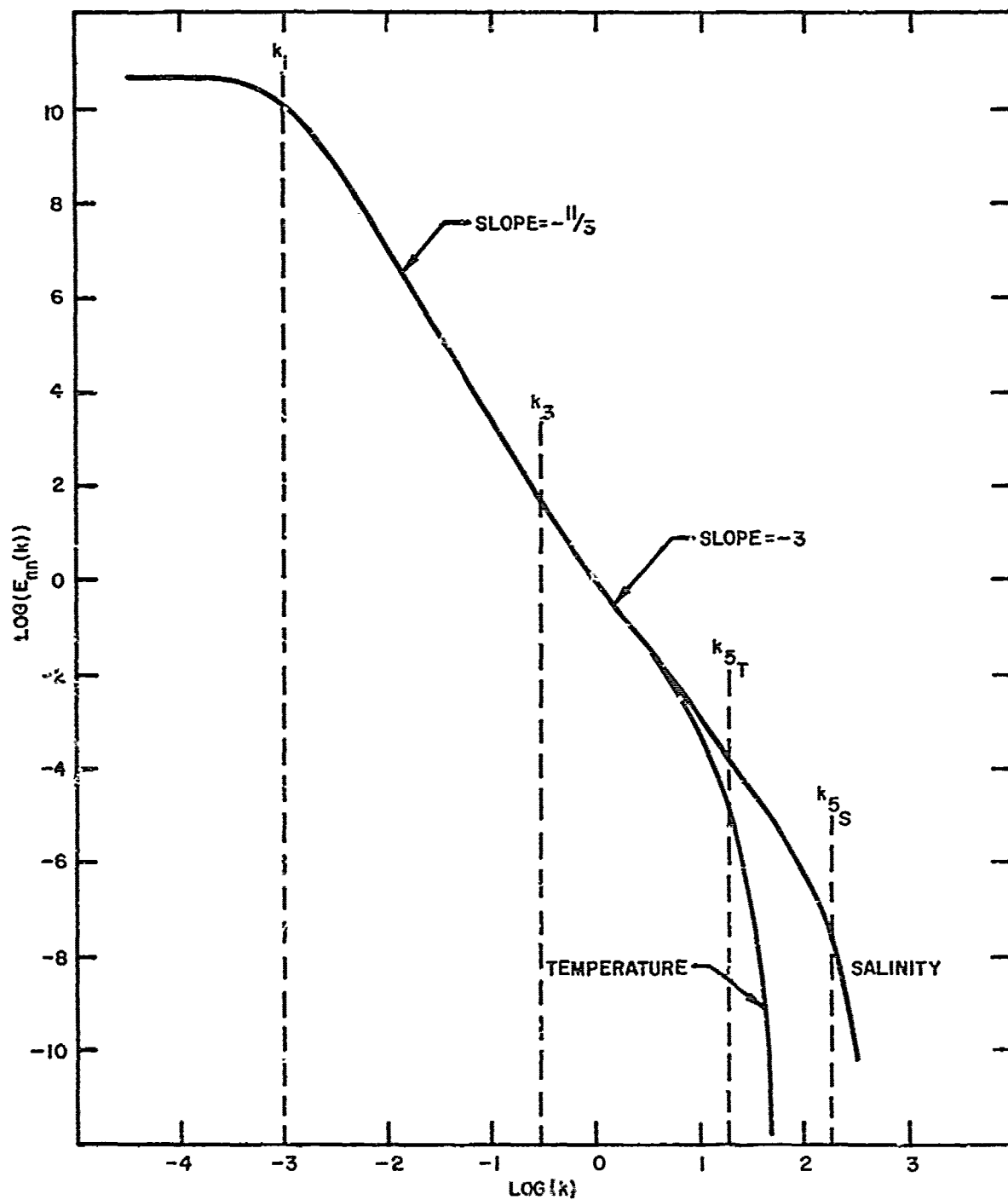


Figure 2
 Three-Dimensional Spectrum of Refractive Index
 Variations, $E_{nn}(k)$, as a Function of Wave Number, k

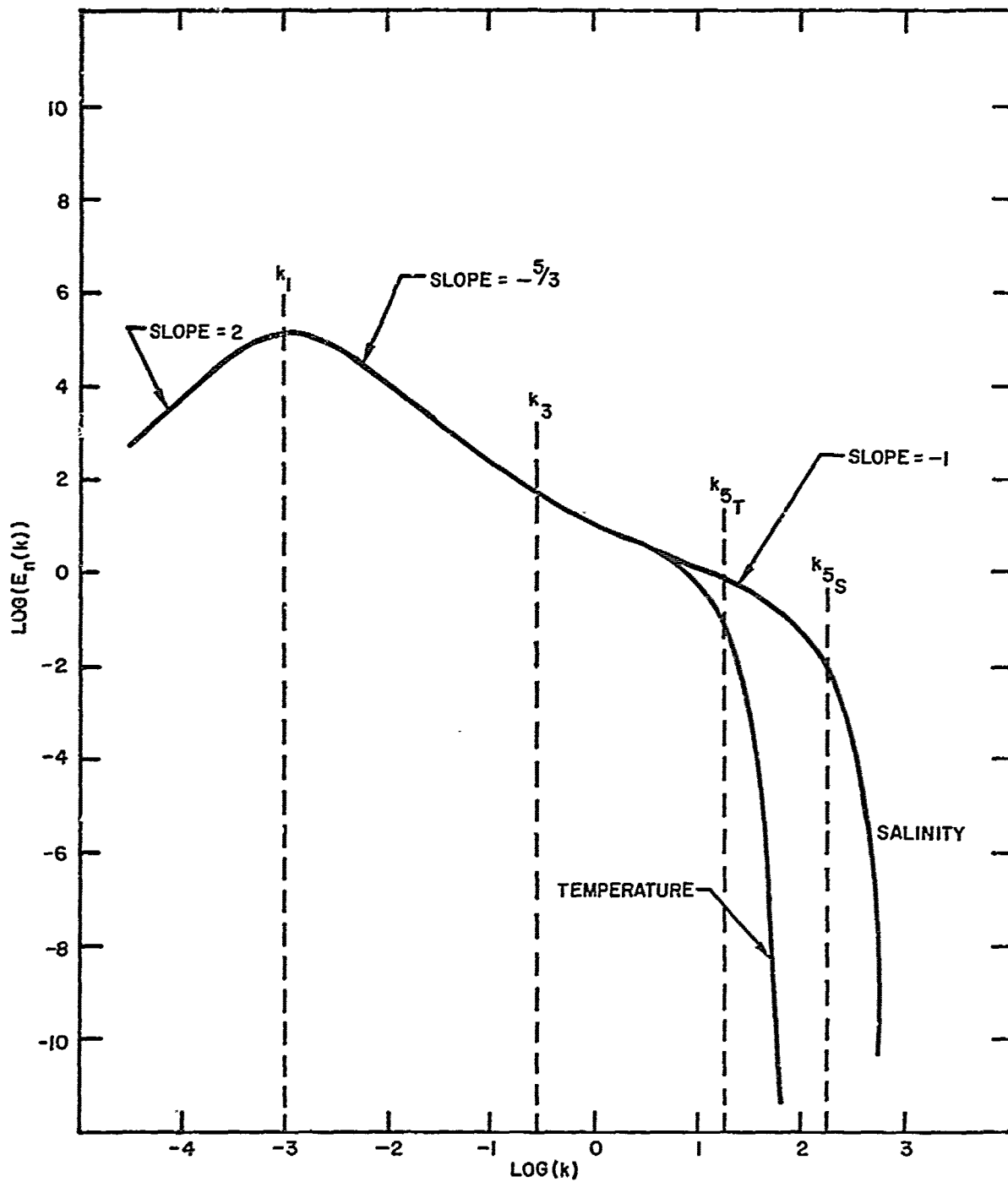


Figure 3
 Modified Three-Dimensional Spectrum of Refractive
 Index Variations, $E_n(k)$, as a Function of Wave Number, k

21

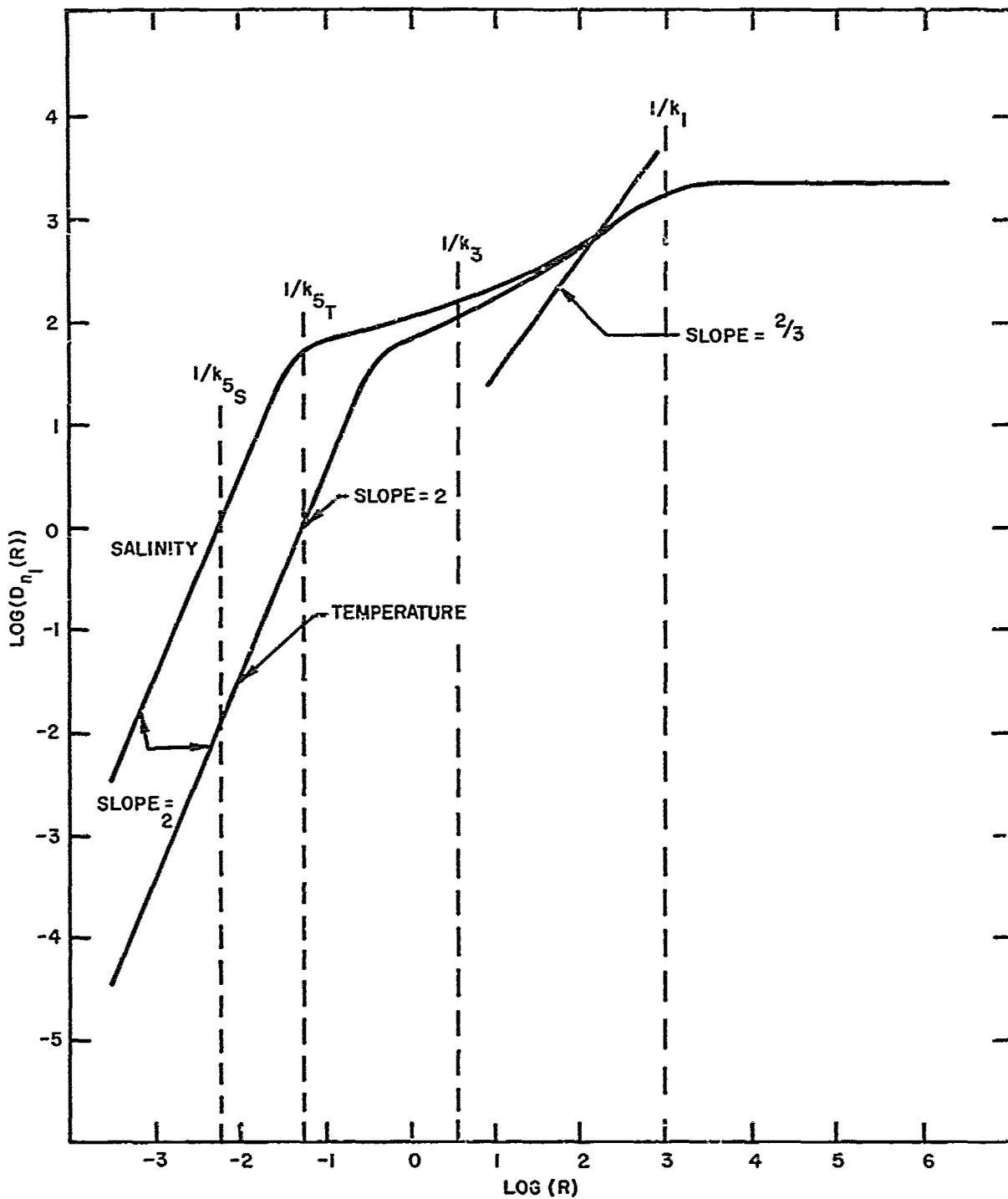


Figure 4
 Structure Function of Refractive Index Variations,
 $D_{n_l}(r)$, as a Function of Distance, r

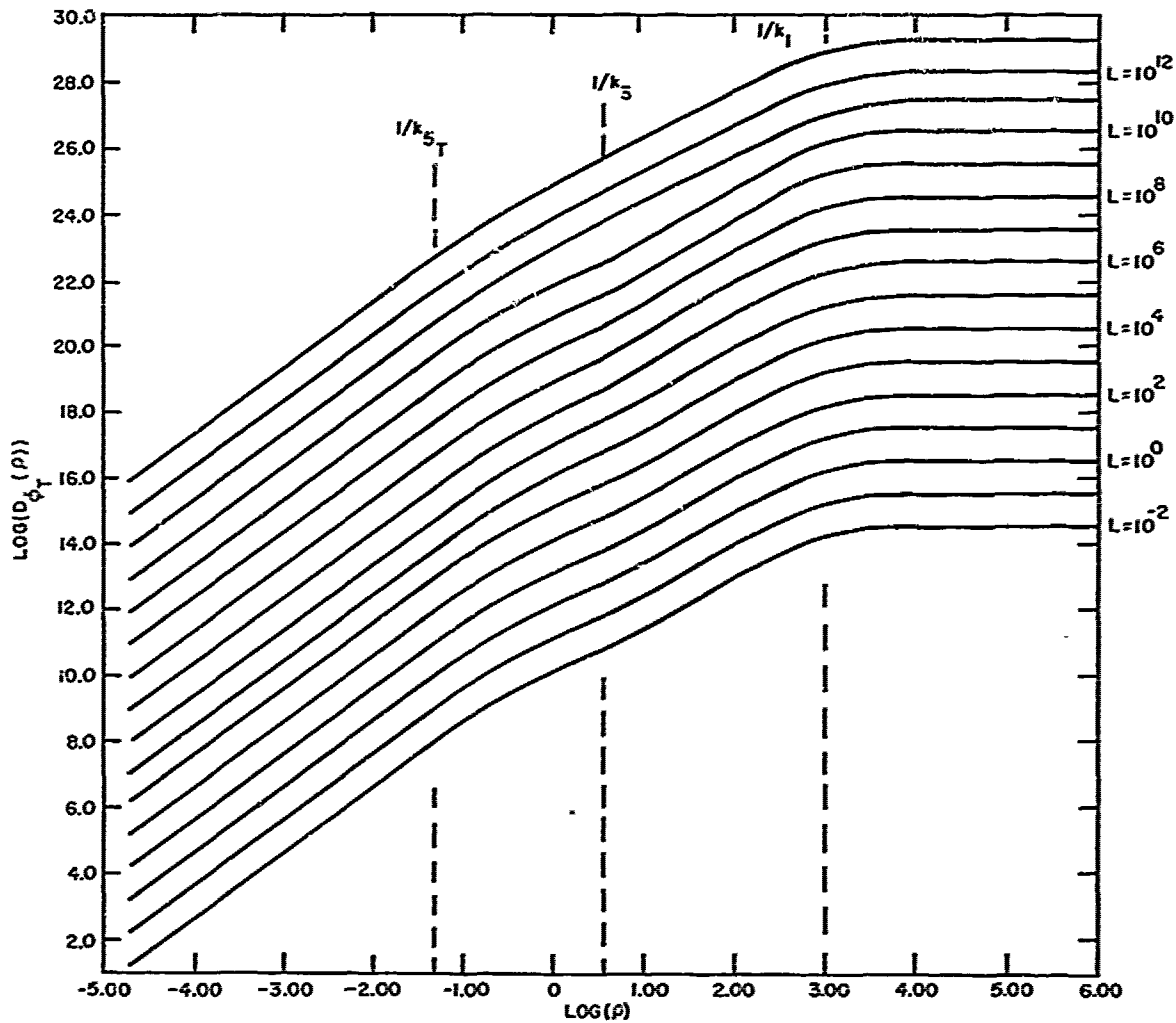


Figure 5
 Computed Phase Structure Function for
 Temperature, $D_{\phi_T}(\rho)$, as a Function of Separation
 Distance, ρ , and Distance Traversed, L

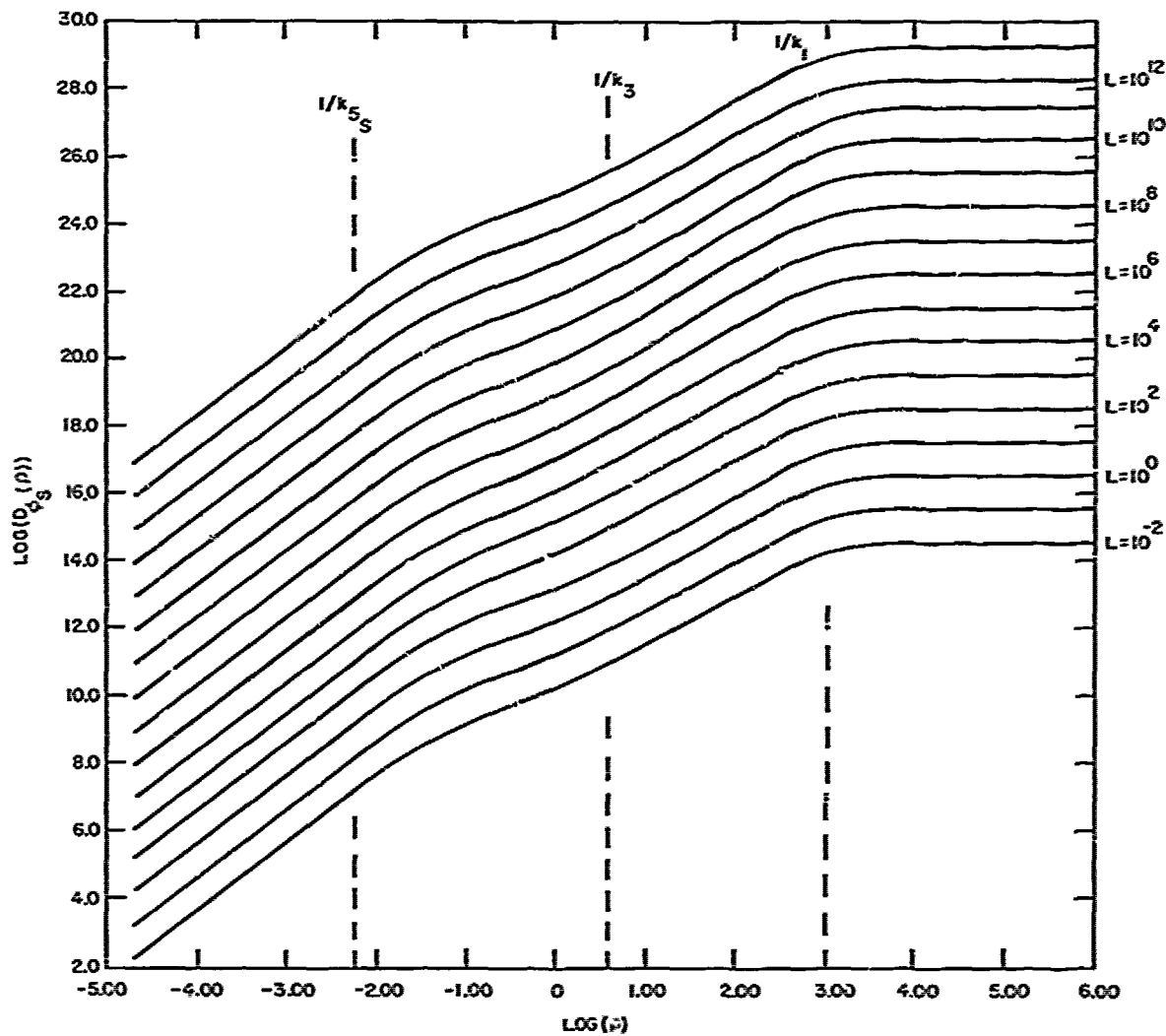


Figure 6
 Computed Phase Structure Function for
 Salinity, $D_{GS}(\rho)$, as a Function of Separation
 Distance, ρ , and Distance Traversed, L

24

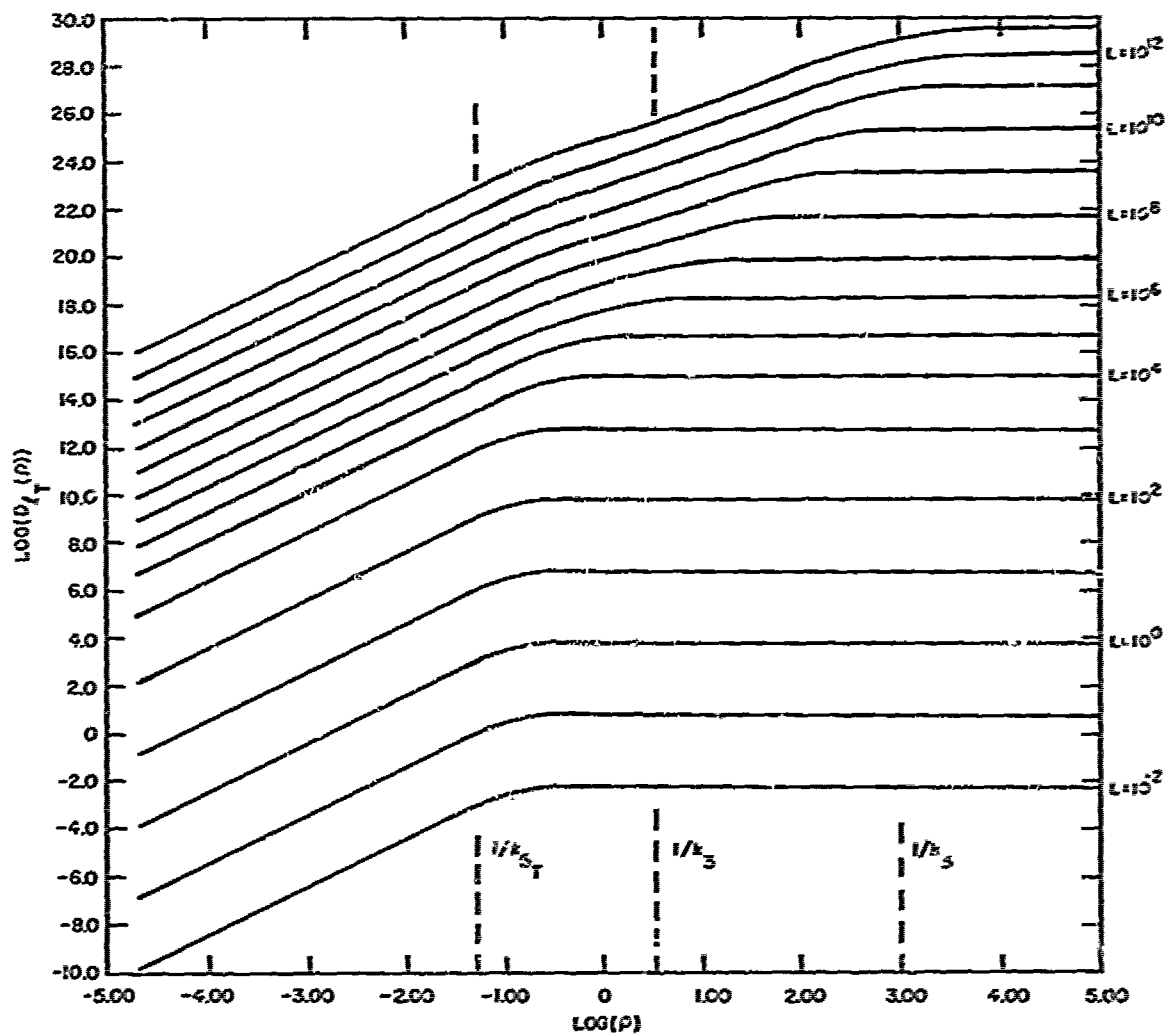


Figure 7
 Computed Logarithmic Amplitude Structure Function for
 Temperature, $D_{gT}(\rho)$, as a Function of Separation
 Distance, ρ , and Distance Traversed, L

25

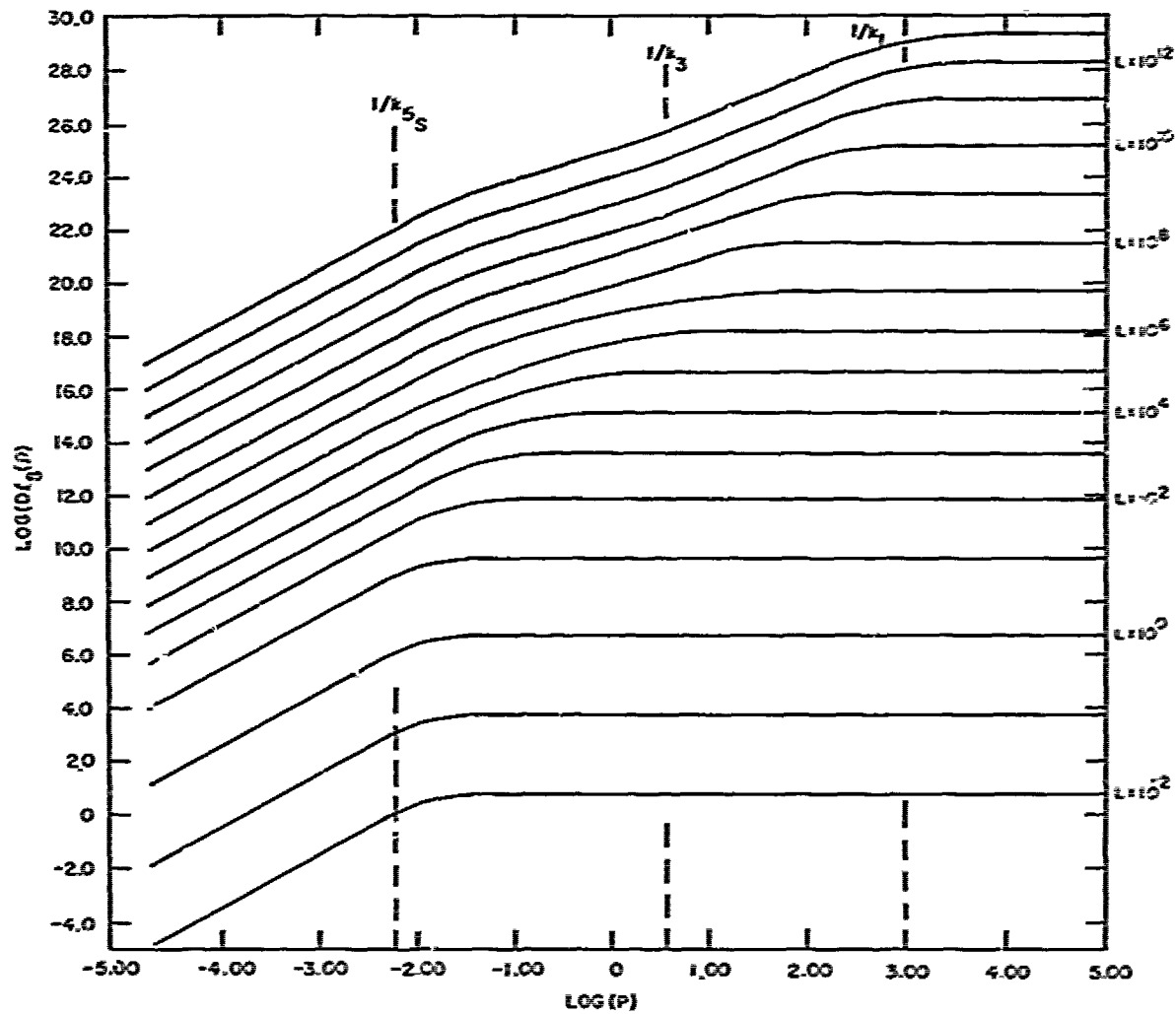


Figure 8
 Computed Logarithmic Amplitude Structure Function for
 Salinity, $D_{1S}(r)$, as a Function of Separation Distance,
 r , and Distance Traversed, L

76

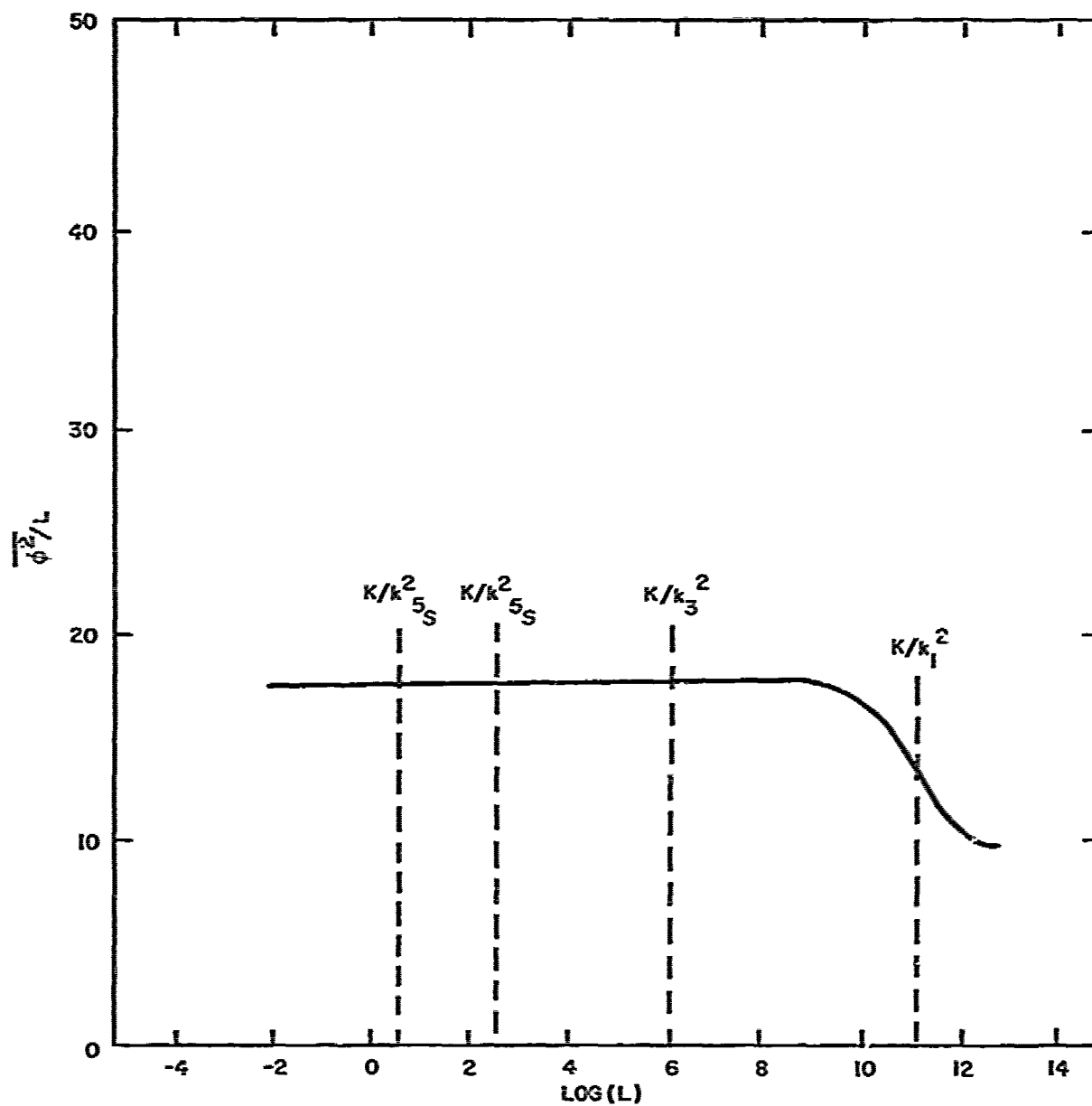


Figure 9
 Length Normalized Optical Phase Variance, $\overline{\phi^2}/L$,
 as a Function of Distance Traversed, L

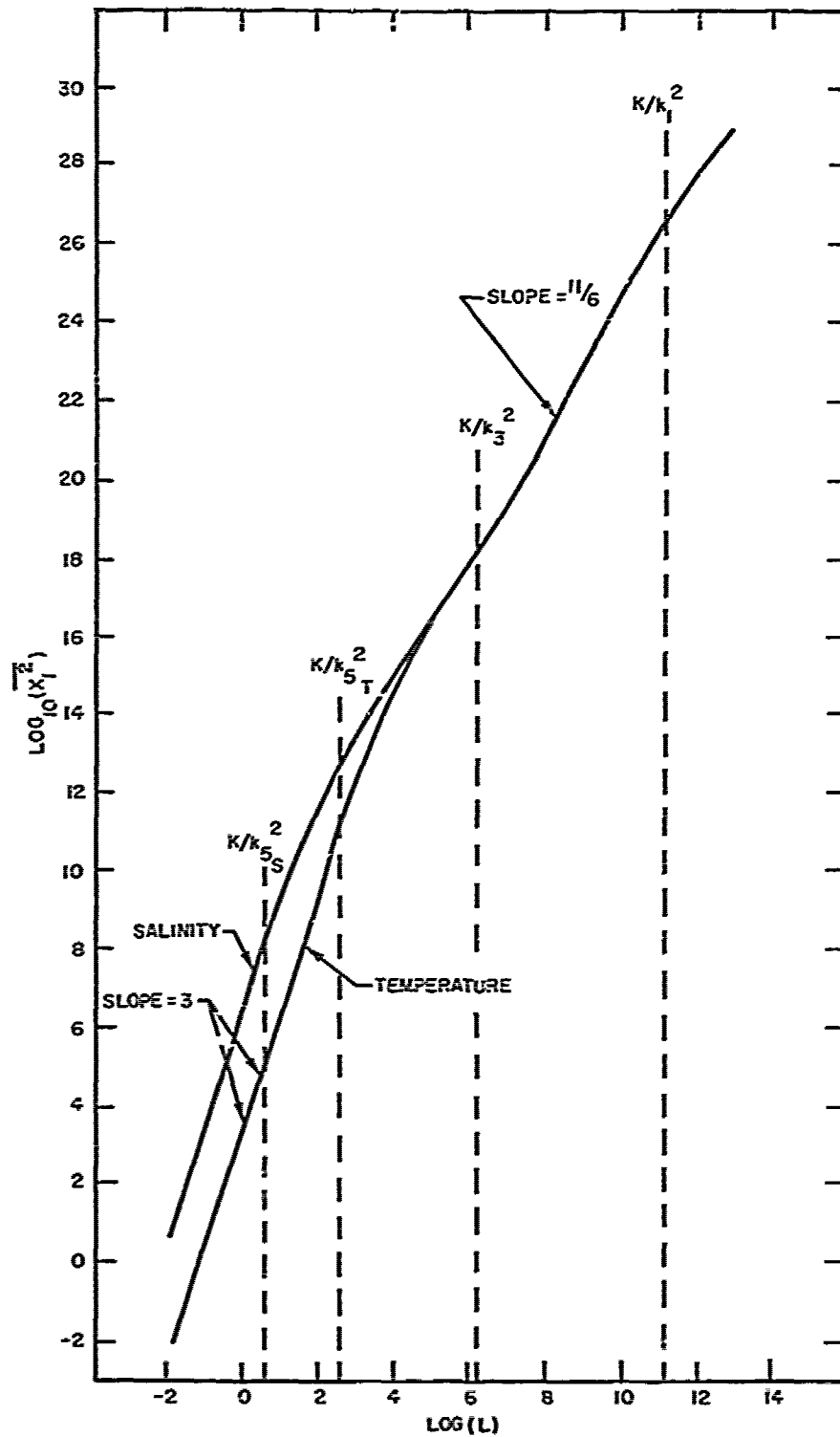


Figure 10
 Optical Intensity Variance, $\overline{X_1^2}$,
 as a Function of Distance Traversed, L

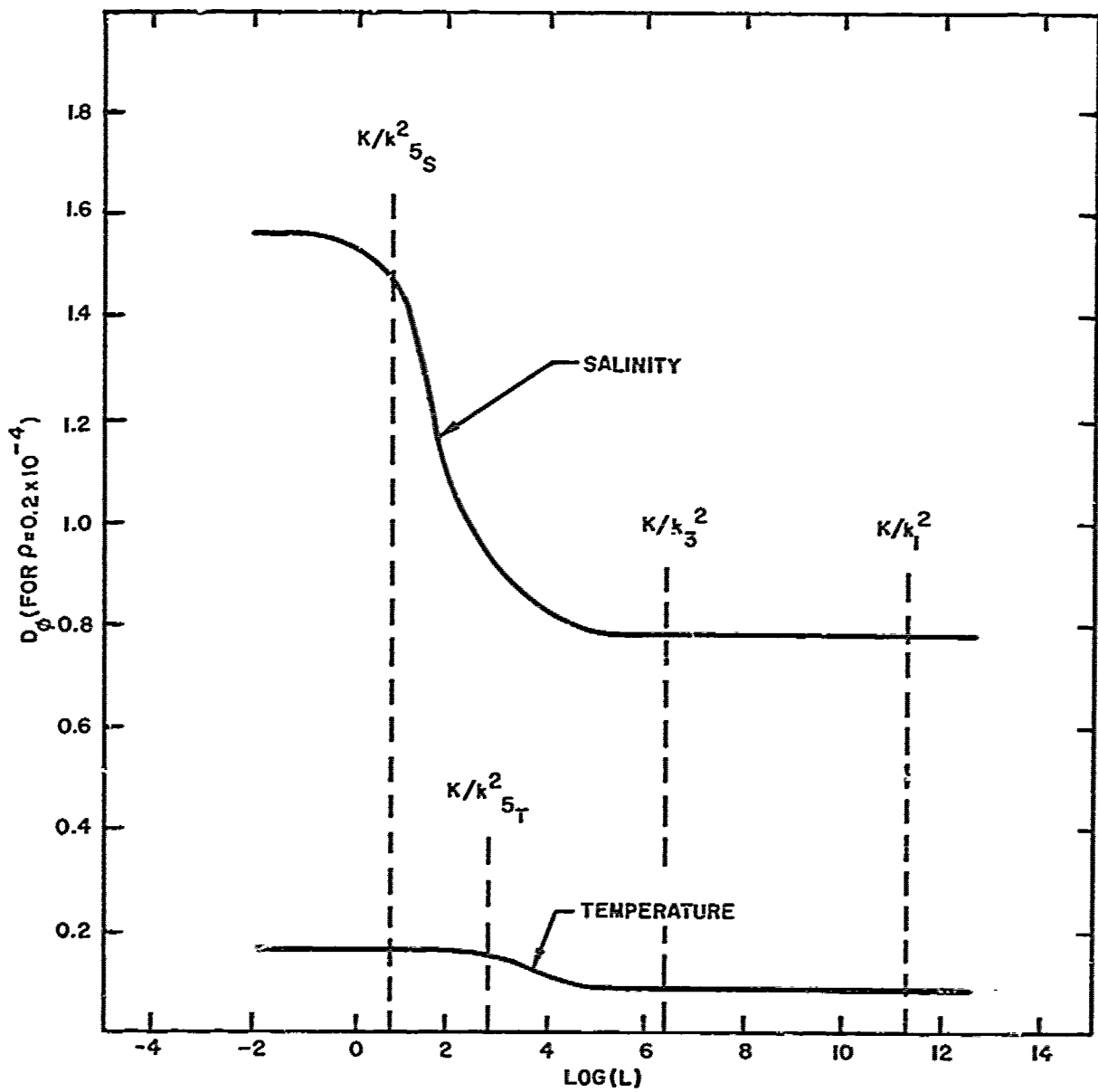


Figure 11
 Optical Phase Structure Function, D_ϕ , at Separation
 Distance $\rho = 0.2 \times 10^{-4}$ as a Function of Distance
 Traversed, L

APPENDIX A

STATISTICAL DESCRIPTIONS OF RANDOM FUNCTIONS AND RANDOM FIELDS

REFERENCES

- (a) Laster, D. R., "Proposed Optical Methods for Measuring Ocean Micro-Scale Turbulence Effects," Marine Sciences Instrumentation, Vol. 4, New York, Plenus Press (1968)
- (b) Gibson, C. H., and W. H. Schwartz, "The Universal Equilibrium Spectra of Turbulent Velocity and Scalar Fields," J. Fluid Mech., Vol. 10, pp. 365-385 (1963)
- (c) Hinze, J. O., Turbulence, New York, McGraw-Hill Book Co. (1959)

LIST OF SYMEOLS

(.)*	Indicates complex conjugate	C(.)	Covariance function
$\overline{(\cdot)}$	Indicates average	D(.)	Structure function
τ, t	Time variables	\vec{r}	Vector distance
ω	Radian frequency	\vec{k}	Vector wave number
$\psi(\cdot)$	Fourier transform of time function	$B_f(\cdot)$	Modified three-dimensional spectrum
$\delta(\cdot)$	Dirac delta function	$B_{ff}(\cdot)$	Three-dimensional spectrum
i	$\sqrt{-1}$	B_{f1}	One-dimensional spectrum
$\{f(t)\}$	Ensemble of functions, $f(t)$	B_{f2}	Two-dimensional spectrum
$m(\cdot)$	Mean		
$B(\cdot)$	Correlation function		

ANALYSIS OF A RANDOM FUNCTION

A set or ensemble of random functions, $\{f_p(t)\}$, can be described by all possible multidimensional probability distributions. In practice, only the mean and the autocorrelation function (the first joint moment) are employed. If the Gaussian distribution applies, the functions are completely described. A priori knowledge or assumptions on the properties of the random function provide different methods for obtaining the descriptive functions.

The mean and the autocorrelation function are given by the expressions in (A-1). The averages here are

$$m_f(t) = \overline{\{f_p(t)\}}$$

$$B_f(t, \tau) = \overline{\{f_p(t) f_p^*(t + \tau)\}} \quad (A-1)$$

where

$f_p(t)$ = the p^{th} realization of the random function at argument t

$m_f(t)$ = the ensemble average at argument t

$B_f(t, \tau)$ = the autocorrelation function at argument t and lag τ .

If $m_f(t)$ and $B_f(t, \tau)$ are independent of t , the ensemble is said to be weakly stationary. If all the probability distributions are independent of t , the ensemble is stationary. If the ensemble is quasi-ergodic, then the mean and autocorrelation functions may be obtained by the expressions in (A-2) employing averaging across any member of the ensemble.

$$m_f = \lim_{T \rightarrow \infty} \frac{1}{T} \int_{-T/2}^{T/2} f(t) dt$$

$$B_f(\tau) = \lim_{T \rightarrow \infty} \frac{1}{T} \int_{-T/2}^{T/2} f(t) f^*(t + \tau) dt \quad (A-2)$$

If all the probability distributions can be obtained by such an average, the ensemble is ergodic. If the properties can be derived from any short-term average (removing the limits of the expressions in (A-2)), the ensemble is referred to as weakly or strongly self-stationary, where the weak connotes the same meaning as in the case of stationarity.

ANALYSIS TECHNIQUES FOR WEAKLY SELF-STATIONARY FUNCTIONS

Where quasi-ergodicity and weak self-stationarity can be assumed, additional descriptions of the function, based on the mean and autocorrelation function are available. Expression (A-3) gives the variance; expression (A-4) gives the covariance function. In the case of a mean free function, the autocorrelation function and the covariance function are equivalent.

$$C_f(0) = B_f(0) - m_f^2 \quad (\text{A-3})$$

$$C_f(\tau) = B_f(\tau) - m_f^2 = \frac{1}{T} \int_0^T (f(t) - m_f)(f(t+\tau) - m_f) dt. \quad (\text{A-4})$$

A stationary function may be represented in terms of a Fourier-Stieltjes integral as shown in expression (A-5).

$$f(t) = \int_{-\infty}^{\infty} e^{i\omega t} d\psi_f(\omega). \quad (\text{A-5})$$

The autocorrelation function can then be written as expression (A-6)

$$\begin{aligned} B_f(t_1 - t_2) &= \overline{f(t_1)f^*(t_2)} = \overline{\int_{-\infty}^{\infty} e^{i\omega_1 t_1} d\psi_f(\omega_1) \int_{-\infty}^{\infty} e^{-i\omega_2 t_2} d\psi_f^*(\omega_2)} \\ &= \iint_{-\infty}^{\infty} e^{i(\omega_1 t_1 - \omega_2 t_2)} \overline{d\psi_f(\omega_1) d\psi_f^*(\omega_2)}. \end{aligned} \quad (\text{A-6})$$

For stationary ensembles, the ensemble average,

$$\overline{d\psi(\omega_1) d\psi^*(\omega_2)},$$

can be written in terms of a power spectra $W_f(\omega_1)$, as expression (A-7).

$$\overline{d\psi(\omega_1) d\psi^*(\omega_2)} = W_f(\omega_1) \delta(\omega_1 - \omega_2) d\omega_1 d\omega_2. \quad (\text{A-7})$$

In the case of weak self-stationarity, $B(t_1 - t_2)$ must depend only on the difference $\tau = t_1 - t_2$, so that the relationship (A-7) can be employed. Thus, the Fourier transform pair relationship between the autocorrelation function and the power spectra, the expressions in (A-8) can be written. As both functions are even, the expressions in (A-9) follow.

$$B_f(\tau) = \int_{-\infty}^{\infty} e^{i\omega\tau} W_f(\omega) d\omega \quad (A-8)$$

$$W_f(\omega) = \frac{1}{2\pi} \int_{-\infty}^{\infty} e^{i\omega\tau} B_f(\tau) d\tau$$

$$B_f(\tau) = 2 \int_0^{\infty} \cos(\omega\tau) W_f(\omega) d\omega \quad (A-9)$$

$$W_f(\omega) = \frac{1}{\pi} \int_0^{\infty} \cos(\omega\tau) B_f(\tau) d\tau.$$

ANALYSIS TECHNIQUES FOR A CLASS OF NONSTATIONARY RANDOM FUNCTIONS

Many random functions descriptive of physical phenomena cannot be assumed to exhibit even weak stationarity. For example, the temperature and salinity of the ocean are characterized by slowly changing means and variances. A technique has been developed whereby a meaningful analysis can be obtained for the class of random functions known to have stationary increments. This will be defined.

In the general case of a nonstationary random function, the autocorrelation is defined (reference (a)) by expression (A-10).

$$B_A(t_1, t_2) = \overline{f(t_1)f^*(t_2)} = \iint_{-\infty}^{\infty} e^{i(\omega_1 t_1 - \omega_2 t_2)} \overline{d\psi_f(\omega_1) d\psi_f^*(\omega_2)}$$

$$= \int_{-\infty}^{\infty} \int_{-\infty}^{\infty} e^{i(\omega_1 t_1 - \omega_2 t_2)} S_A(f_1, f_2) df_1 df_2. \quad (\text{A-10})$$

It is desirable here to make the variable changes defined by the expression in (A-11) which provide the definitions of the expressions in (A-12).

$$\left. \begin{aligned} \tau &= t_1 - t_2 & t &= \frac{t_1 + t_2}{2} \\ t_1 &= t - \tau/2 & t_2 &= t + \tau/2 \\ f &= f_1 - f_2 & g &= \frac{f_1 + f_2}{2} \\ f_1 &= g - f/2 & f_2 &= g + f/2 \end{aligned} \right\} \quad (\text{A-11})$$

$$\left. \begin{aligned} B_B(\tau, t) &= B_A(t_1, t_2) \\ S_B(f, g) &= S_A(f_1, f_2) \end{aligned} \right\} \quad (\text{A-12})$$

The expressions in (A-10) and (A-12) provide the expressions in (A-13).

$$B_B(\tau, t) = \int_{-\infty}^{\infty} \int_{-\infty}^{\infty} e^{i2\pi(f\tau - gt)} S_B(f, g) df dg$$

$$S_B(f, g) = \int_{-\infty}^{\infty} \int_{-\infty}^{\infty} e^{-i2\pi(f\tau - gt)} B_B(t, \tau) dt d\tau. \quad (\text{A-13})$$

If $f(t)$ were stationary, the expressions in (A-14) must hold to satisfy expression (A-8).

$$B_f(\tau) = B_B(\tau, t) \delta(t) \tag{A-14}$$

$$W_f(f) = S_B(f, g) \delta(g).$$

The Dirac delta functions of the expressions in (A-14) show the lack of dependence on t_1 and t_2 . If this lack of dependence occurs only over a range $\tau < \tau_0$, the expressions in (A-12) can be approximated (reference (b)) as shown by expressions in (A-15).

$$B_B(\tau, t) = B_1(\tau) B_2(t); \quad \tau < \tau_0 \tag{A-15}$$

$$S_B(f, g) = S_1(f) S_2(g); \quad f < 1/\tau_0$$

The applicability of this approximation can be demonstrated. This leads to a practical method for obtaining stable information about the random function in question.

Consider a mean-free, random function with a slowly varying multiplicative scale factor. The variance, for example, is varying with this factor. The stationary variations can be separated if the scale length of the variations of the scale factor is $\tau > \tau_0$, where $\tau_0 > \tau_1$, the scale length which includes the stationary variations. A correlation of the form given in expression (A-10) performed at some $t = t_a$ will have the same form as one performed at $t = t_b$ except for a scale factor. All such correlations will be 0 for $\tau_1 < \tau < \tau_0$. At $\tau > \tau_0$, the approximation no longer holds, and a deviation from zero occurs. Thus, the correlation function of the stationary variations can be obtained, and the scale length of the nonstationarity can be determined.

Difficulty occurs if the random function contains a non-stationary mean. Correlations of the form of expression (A-10) cannot be usefully employed. The average of expression (A-16) provides a method of analysis.

$$\overline{[f(t_1) - f(t_2)]^2} = B_B(0, t - \tau/2) + B_B(0, t + \tau/2) - 2B_B(\tau, t). \quad (\text{A-16})$$

An important feature of the average of expression (A-16) is that any variations in the mean of scale length greater than $\tau = t_2 - t_1$ will not affect the result. Thus, expression (A-16) can be treated as if the random function, $f(t)$, were mean free and expression (A-17) can be written for τ less than the scale length of the variations of the mean.

$$\overline{[f(t_1) - f(t_2)]^2} = B_1(0) B_2(t - \tau/2) + B_2(t + \tau/2) - 2B_1(\tau)B_2(t). \quad (\text{A-17})$$

Expression (A-18) can be written

$$E_2(t - \tau/2) = B_2(t) = B_2(t + \tau/2); \quad \tau < \tau_0 \quad (\text{A-18})$$

if the scale length of the variations of the scale factor exceeds τ_0 . Finally, expression (A-19) can be written if the scale length of the variations of the mean and the scale factor (variance) exceed τ_0 .

$$\overline{[f(t_1) - f(t_2)]^2} = 2B_2(t) [B_1(0) - B_1(\tau)]; \quad \tau < \tau_0 \quad (\text{A-19})$$

If the average of expression (A-19) is evaluated at different t 's, the result will remain τ invariant. If the scale length of the stationary variations is $\tau_1 < \tau_0$, the result will be zero at $\tau = 0$, a constant for $\tau_1 < \tau < \tau_0$, and will deviate from the constant for $\tau > \tau_0$. Generally, a random function which can be analyzed in this manner is said to have stationary increments.

The average introduced by expression (A-16) is referred to as the structure function (reference (c)). The expressions in (A-20) define this function using the definitions of the expressions in (A-11).

$$D_A(t_1 t_2) = D_B(\tau, t) = \overline{[f(t_1) - f(t_2)]^2}$$

$$= D_f(t, \tau). \quad (A-20)$$

SUMMARY OF MOST OFTEN EMPLOYED ANALYSIS TECHNIQUES

The most often employed analysis techniques are summarized in this section. It will be assumed that the random function is at least weakly self-stationary except for nonstationarities in mean and a scale factor (variance). Quasi-ergodicity is then also assumed.

Mean and Variance

The mean is calculated as shown in expression (A-21):

$$m_f = \frac{1}{T} \int_0^T f(t) dt. \quad (A-21)$$

T is chosen based on the scale length of the period of the lowest "stationary" variation.

The variance is calculated as shown in expression (A-22).

$$C_f(0) = \frac{1}{T} \int_0^T f^2(t) dt - m_f^2. \quad (A-22)$$

T must be chosen as expressed above.

Autocorrelation and Covariance Functions

The autocorrelation function is calculated as shown in expression (A-23).

$$B_f(\tau) = \frac{1}{T} \int_0^T f(t) f^*(t + \tau) dt. \quad (\text{A-23})$$

Again T must be carefully chosen. The covariance function is calculated as shown by the expression (A-24).

$$\begin{aligned} C_f(\tau) &= \frac{1}{T} \int_0^T (f(t) - m)(f(t + \tau) - m)^* dt \\ &= B_f(\tau) - m^2. \end{aligned} \quad (\text{A-24})$$

Thus, for mean-free random functions, the correlation and covariance are equivalent. In the case of nonstationarities in mean and scale factor (variance), particularly if the mean is large as compared to the variance, expressions (A-22), (A-23), and (A-24) may not provide useful results.

Structure Function

Expression (A-25) defines the structure function.

$$D_f^i(\tau) = \frac{1}{T} \int_0^T [f(t) - f(t + \tau)]^2 dt. \quad (\text{A-25})$$

T is determined as expressed above. The structure function to be most often employed is defined by the expressions in (A-26), where τ_0 is the scale length described above.

$$D_f(\tau) = D_f^i(\tau); \quad \tau \leq \tau_0 \quad (\text{A-26})$$

$$D_f(\tau) = D_f^i(\tau_0); \quad \tau \geq \tau_0.$$

The definitions of the expressions in (A-26) provide a methodology of defining a mean-free autocorrelation function in terms of the structure function which can be universally applied in later analysis. This is shown in the expressions in (A-27).

$$\begin{aligned} D_f(\tau) &= 2[B_f(0) - B_f(\tau)] \\ D_f(\alpha) &= 2B_f(0) = 2C_f(0) \\ B_f(\tau) &= 1/2[D_f(\alpha) - D_f(\tau)] \end{aligned} \tag{A-27}$$

Spectral Functions

The expressions in (A-28) were given above as expressions (A-9).

$$\begin{aligned} B_f(\tau) &= 2 \int_0^{\infty} \cos(\omega\tau) W_f(\omega) d\omega \\ W_f(\omega) &= \frac{1}{\pi} \int_0^{\infty} \cos(\omega\tau) B_f(\tau) d\tau. \end{aligned} \tag{A-28}$$

The expressions in (A-29) relating the structure function to the spectral function, follow from expression (A-28) and the definitions of expressions (A-27).

$$\begin{aligned} D_f(\tau) &= 4 \int_0^{\infty} (1 - \cos(\omega\tau)) W_f(\omega) d\omega \\ W_f(\omega) &= \frac{D_f(\alpha)}{2} \delta(\omega) - \frac{1}{2\pi} \int_0^{\infty} \cos(\omega\tau) D_f(\tau) d\tau. \end{aligned} \tag{A-29}$$

ANALYSIS OF RANDOM FIELDS

A random function of three variables is a random field. Only scalar fields are considered here. A random field is considered homogeneous if its mean value is constant and autocorrelation does not change with position. The expressions in (A-30) show these results.

$$\overline{f(\vec{r})} = \text{constant} \tag{A-30}$$

$$B_f(\vec{r}_1, \vec{r}_2) = B_f(\vec{r}_1 + \vec{r}_0, \vec{r}_2 + \vec{r}_0).$$

Setting $\vec{r}_0 = -\vec{r}_2$ in expression (A-30) provides the expressions in (A-31).

$$B_f(\vec{r}_1, \vec{r}_2) = B_f(\vec{r}_1 - \vec{r}_2, 0) = B_f(\vec{r}_1 - \vec{r}_2) = B_f(\vec{r}). \tag{A-31}$$

Expression (A-31) shows that homogeneity corresponds to weak stationarity in random functions.

If $B_f(\vec{r})$ depends only on $|\vec{r}| = r$, the random field is isotropic. Thus, isotropy corresponds to quasi-ergodicity.

A random field may be represented by a Fourier-Stieltjes integral as shown by expression (A-32).

$$f(\vec{r}) = \iiint_{-\infty}^{\infty} \exp(i\vec{k} \cdot \vec{r}) d\psi_f(\vec{k}). \tag{A-32}$$

The autocorrelation function can then be written as shown by the expressions in (A-33).

$$B_f(\vec{r}) = f(\vec{r}_1) \overline{f(\vec{r}_2)}$$

$$= \iiint_{-\infty}^{\infty} \iiint_{-\infty}^{\infty} \exp[i(\vec{k}_1 \cdot \vec{r}_1 - \vec{k}_2 \cdot \vec{r}_2)] \overline{d\psi_f(\vec{k}_1) d\psi_f^*(\vec{k}_2)}$$

$$= \iiint_{-\infty}^{\infty} \exp(i\vec{k} \cdot \vec{r}) E_{ff}(\vec{k}) d\vec{k} \quad (\text{A-33})$$

where

$$\overline{d\psi_f(\vec{k}_1) d\psi_f^*(\vec{k}_2)} = \delta(\vec{k}_1 - \vec{k}_2) E_{ff}(\vec{k}_1) d\vec{k}_1 d\vec{k}_2.$$

Considering the even characteristic of the functions, the expressions in (A-34) show the Fourier transform pair relationship between the autocorrelation and the three-dimensional spectrum.

$$B_f(\vec{r}) = \iiint_{-\infty}^{\infty} \cos(\vec{k} \cdot \vec{r}) E_{ff}(\vec{k}) d\vec{k} \quad (\text{A-34})$$

$$E_{ff}(\vec{k}) = \left(\frac{1}{2\pi}\right)^3 \iiint_{-\infty}^{\infty} \cos(\vec{k} \cdot \vec{r}) B_f(\vec{r}) d\vec{r}.$$

ISOTROPIC HOMOGENEOUS RANDOM FIELDS

If the random field is isotropic and homogeneous on a plane $x = \text{const}$, the autocorrelation can be expressed in terms of a two-dimensional spectrum which can be related to the three-dimensional spectrum. This is developed in the expressions in (A-35).

$$B_f(x, \rho) = \int_{-\infty}^{\infty} \int_0^{\infty} \int_0^{2\pi} d\theta k_\rho dk_\rho dk_x \cos(k_x x + k_\rho \rho \cos\theta) E_{ff}(k_\rho, k_x)$$

$$= \int_{-\infty}^{\infty} \int_0^{\infty} \int_0^{2\pi} d\theta k_\rho dk_\rho dk_x [\cos(k_x x) \cos(k_\rho \rho \cos\theta) - \sin(k_x x) \sin(k_\rho \rho \cos\theta)] E_{ff}(k_\rho, k_x)$$

(As E_{ff} is even)

$$= \int_{-\infty}^{\infty} \int_0^{\infty} \int_0^{2\pi} d\theta k_{\rho} dk_{\rho} dk_x \cos(k_x x) \cos(\rho k_{\rho} \cos\theta) E_{ff}(k_{\rho}, k_x)$$

$$\text{(As } 2\pi J_0(k_{\rho} \rho) = \int_0^{2\pi} \cos(k_{\rho} \rho \cos\theta) d\theta$$

$$= 2\pi \int_{-\infty}^{\infty} \int_0^{\infty} \cos(k_x x) J_0(k_{\rho} \rho) E_{ff}(k_{\rho}, k_x) k_{\rho} dk_{\rho} dk_x$$

$$= 2\pi \int_0^{\infty} dk_{\rho} k_{\rho} J_0(k_{\rho} \rho) \int_{-\infty}^{\infty} dk_x E_{ff}(k_{\rho}, k_x) \cos(k_x x)$$

$$= 2\pi \int_0^{\infty} dk_{\rho} k_{\rho} J_0(k_{\rho} \rho) E_{f2}(k_{\rho}, x).$$

(A-35)

The final expression shows the two dimensional spectrum, $E_{f2}(k_{\rho}, x)$. The Fourier transform relationship to the three-dimensional spectrum is shown in expression (A-36).

$$E_{f2}(k_{\rho}, x) = \int_{-\infty}^{\infty} \cos(k_x x) E_{ff}(k_x, k_{\rho}) dk_x$$

(A-36)

$$E_{ff}(k_x, k_{\rho}) = \frac{1}{2\pi} \int_{-\infty}^{\infty} E_{f2}(k_{\rho}, x) \cos(k_x x) dx.$$

Further insight into the two-dimensional spectrum is shown by the expressions in (A-37).

$$f(x, y, z) = \int_{-\infty}^{\infty} \int_{-\infty}^{\infty} \exp[i(k_y y + k_z z)] d_{f2}(k_y, k_z, x)$$

$$\delta(k_2 - k_2') \delta(k_3 - k_3') E_{f2}(k_y, k_z, x) dk_y dk_z dk_y' dk_z'$$

$$= d\psi_{f2}(k_y, k_z, x) d\psi_{f2}^*(k_y', k_z', x). \quad (A-37)$$

The first of these shows the random field on the plane $x = \text{const}$ expanded in a Fourier-Stieltjes integral. The second expression shows the two-dimensional spectrum in terms of that expansion.

If the random field is homogeneous, the correlation function and the two-dimensional spectrum are independent of x as shown in the expressions in (A-38).

$$B_f(\rho) = 2\pi \int_0^{\infty} dk_{\rho} k_{\rho} J_0(k_{\rho} \rho) E_{f2}(k_{\rho})$$

$$E_{f2}(k_{\rho}) = \int_{-\infty}^{\infty} E_{ff}(k_x, k_{\rho}) dk_x. \quad (A-38)$$

If the random field is homogeneous and isotropic, the auto-correlation can be expressed in terms of a one-dimensional power spectrum which can be expressed in terms of the three-dimensional spectrum. This is developed in the expressions in (A-39).

$$\begin{aligned}
B_{ff}(k_r) &= \frac{1}{(2\pi)^3} \int_{-\infty}^{\infty} \int_0^{\pi} \int_{-\pi/2}^{\pi/2} \cos(k_r r \cos\theta) B_f(r) (r \sin\theta d\theta) (r d\theta) dr \\
&= \frac{1}{2(2\pi)^2} \int_{-\infty}^{\infty} \int_0^{\pi} \cos(k_r r \cos\theta) B_f(r) r^2 \sin\theta d\theta dr \\
&= \frac{1}{2(2\pi)^2} \int_{-\infty}^{\infty} dr \frac{r}{k_r} \int_0^{\pi} B_f(r) \frac{d}{d\theta} \left[-\sin(k_r r \cos\theta) \right] d\theta \\
&= \frac{1}{(2\pi)^2} \int_{-\infty}^{\infty} dr \frac{r}{k_r} B_f(r) \sin(k_r r) \\
&= \left(\frac{1}{2\pi k_r} \right) \left[-\frac{\partial}{\partial k_r} \frac{1}{2\pi} \int_{-\infty}^{\infty} dr \cos(k_r r) B_f(r) \right] \\
&= \frac{-1}{2\pi k_r} \frac{2}{2k_r} E_{f1}(k_r) \tag{A-39}
\end{aligned}$$

and

$$\begin{aligned}
E_{ff}(k_r) &= \frac{1}{2\pi^2 k_r} \int_0^{\infty} r B_f(r) \sin(k_r r) dk_r \\
B_f(r) &= \frac{4\pi}{r} \int_0^{\infty} k_r E_{ff}(k_r) \sin(k_r r) dk_r.
\end{aligned}$$

The expressions in (A-39) show that one-dimensional spectrum exhibits the expected Fourier transform relationships of the expressions in (A-40).

$$E_{fl}(k_r) = \frac{1}{2\pi} \int_{-\infty}^{\infty} dr \cos(k_r r) B_f(r)$$

$$B_f(r) = \int_{-\infty}^{\infty} dk_r \cos(k_r r) E_{fl}(k_r) \quad (A-40)$$

In addition, expression (A-41) may be written

$$E_{fl}(k_r) = \int_{k_r}^{\infty} dk (2\pi k) \bar{E}_{ff}(k) + \int_{-k_r}^{\infty} dk (2\pi k) E_{ff}(k)$$

$$= \int_{k_r}^{\infty} dk (4\pi k) \bar{E}_{ff}(k) \quad (A-41)$$

All the results of previous sections defining relationships between the autocorrelation and power spectral functions apply to the autocorrelation, $B_f(r)$, and the one-dimensional spectrum $E_{fl}(r)$.

LOCALLY HOMOGENEOUS AND ISOTROPIC RANDOM FIELDS

The methodology of previous sections on local stationarity is applied to locally homogeneous random fields. The three-dimensional structure function is defined by expression (A-42).

$$D_f(\vec{r}_1, \vec{r}_2) = \overline{[f(\vec{r}_1) - f(\vec{r}_2)]^2} \quad (A-42)$$

The field is locally homogeneous if shifts of \vec{r}_1 and \vec{r}_2 within a region do not change the structure function as shown in expression (A-43).

$$D_f(\vec{r}_1 + \vec{r}_0, \vec{r}_2 + \vec{r}_0) = D_f(\vec{r}_1, \vec{r}_2) = D_f(\vec{r}_1 - \vec{r}_2). \quad (\text{A-43})$$

In case of local homogeneity and isotropy on a plane $x = \text{const}$, expression (A-44) results.

$$D_f(\rho) = 4\pi \int_0^{\infty} [1 - J_0(k_\rho \rho)] E_{f2}(k_\rho, 0) k_\rho dk_\rho. \quad (\text{A-44})$$

In the case of local homogeneity and isotropy, expression (A-45) results.

$$\begin{aligned} D_f(r) &= 2 \int_{-\infty}^{\infty} (1 - \cos k_r r) E_{f1}(k_r) dk_r \\ &= 4\pi \int_{-\infty}^{\infty} \left[1 - \frac{\sin k_r r}{k_r r} \right] E_{ff}(k_r) k_r^2 dk_r. \end{aligned} \quad (\text{A-45})$$

The one-, two-, and three-dimensional spectra are related as above except that no Dirac delta exists for the mean. The structure and correlation functions are considered modified as expressed above for large ρ and r .

The term $4\pi k_r^2 E_{ff}(k_r)$ or, in general, $4\pi k^2 E_{ff}(k)$ seen in the last of expression (A-45), is employed often. For simplicity,

the definition of expression (A-46) is employed. $E_f(k)$ is referred to as the modified three-dimensional spectrum.

$$E_f(k) = 4\pi k^2 E_{ff}(k). \quad (A-46)$$

APPENDIX B

COMPUTER PROGRAM FOR CALCULATING THE OPTICAL PROPAGATION PROPERTIES

This program is utilized for all four of the required calculations. A particular calculation is obtained by changing lines 17 and 19 in the program. In line 17: ICODE = -1, logarithmic amplitude variations are calculated; if ICODE = +1, phase variations. Line 19 sets the k_5 factor; thus XKS = 18 for temperature; XKS = 180 for salinity.

The program provides both printed results and a control tape for a plotter to provide plotted results.

CAPNOPT.T3000,TP1,P3.
CHARGE,CARW.184200601,PR,R.
ATTACH(SCORS,CASGSCORS,ID=289001202)
REQUEST,TAPE48,HI,S.(CA0343/RINGIN)
FTN(T)
REDUCE.
LOAD(SCORS)
LGO.

842.WYBRANIEC

UNLOAD(TAPE48)
00000000000000000000000000000000
PROGRAM OPTCL(OUTPUT,TAPE6=OUTPUT,TAPE48,INPUT,TAPE5=INPUT)
COMMON ICODE,XL,XK5,RHO
DIMENSION W(85),XRHO(85),EE(4),DD(4),TITLE(8)
CALL CAMRAV(35)
READ(5,10) (TITLE(I),I=1,8)
10 FORMAT(A10)
XMIN=-5.
XMAX=6.
YMIN=2.
YMAX=30.
DX=1.
DY=1.
CALL SETMIV(24,0,100,24)
CALL GRIDIV(0,XMIN,XMAX,YMIN,YMAX,DX,DY,0,0,-1,-2,4,4)
CALL PRINTV(80,TITLE,150,24)
PI=3.141592
ICODF=1
RMAX=1000.
X5=130.
IJK=1
I(1)=1.8
WRITE(6,101)
101 FORMAT(1H1)
WRITE(6,102)
102 FORMAT(1H * L RHO DPHIS190*)
WRITE(6,103)
103 FORMAT(1H)
XL=1.E-2
DO 5 I5=1,16
JJ=0
EXP0=1.E-5
DO 6 I6=1,11
DO 7 I7=1,5
JJ=JJ+1
RHO=2.*I7*EXP0
XRHO(JJ)=RHO
DD(1)=.0019
SUM=0.
A=0.
B=A+DD(IJK)
47 AA=.5*(A+B)
BB=B-A
CC=.4801449*BB
Y=.05061427*(FUNC(AA+CC)+FUNC(AA-CC))
CC=.3983337*BB
Y=Y+.1111905*(FUNC(AA+CC)+FUNC(AA-CC))
CC=.2627662*BB
Y=Y+.1568533*(FUNC(AA+CC)+FUNC(AA-CC))
CC=.09171732*BB
Y=BB*(Y+.1813419*(FUNC(AA+CC)+FUNC(AA-CC)))

```

SUM=SUM+Y
IF (9-RMAX) 46,46,48
46 DD(IJK)=DD(IJK)*EE(IJK)
A=R
R=A+DD(IJK)
GO TO 47
48 W(JJ)=4.*PI*SIM
WRITE(6,4) XL,RHO,W(JJ)
4 FORMAT(1H,ER.1,2X,ER.1,2X,E12.5)
7 CONTINUE
EXP0=EXP0*10.
6 CONTINUE
WRITE(6,104)
104 FORMAT(1H )
XRHO(1)=ALOG10(XRHO(1))
W(1)=ALOG10(W(1))
DO 11 I1=1,54
I12=I1+1
XRHO(I12)=ALOG10(XRHO(I12))
W(I12)=ALOG10(W(I12))
IX1=IXV(XRHO(I11))
IX2=IXV(XRHO(I12))
IY1=IYV(W(I11))
IY2=IYV(W(I12))
CALL LINEV(IX1,IY1,IX2,IY2)
11 CONTINUE
XL=XL*10.
5 CONTINUE
CALL PLTND(0)
STOP
END
FUNCTION FUNC(XKP)
COMMON ICODE,XL,XKS,RHO
XK1=.001
XK3=.28
XK=.13236156
PI=3.141592
Z=176.
O1=-2.*(XKP/XK5)**2
IF (7-ABS(O1)) 32,31,31
32 ENN=0.
GO TO 34
31 ENN=((XK3**(2./3.)/XK**(11./3.))*1./((1.+(XK1/XKP)**2)**(11./6.)
1)-1./((1.+(XK3/XKP)**2)**(11./6.)))+(1./((XKP**2+XK3**2)**(3./2.))
2)*EXP(O1)
34 X=XKP**2*XL/XK
CALL CALSIN(X,AMINUS)
IF(ICODE) ?1,21,22
21 E2=PI*(XK**2)*XL*AMINUS*ENN
GO TO ?3
22 APLUS=?.-AMINUS
E2=PI*(XK**2)*XL*APLUS*ENN
23 ARG=XKP*RHO
CALL RES(ARG,SUM)
FUNC=(1.-SUM)*E2*XKP
IF(ARG.LT..1) FUNC=SUM*E2*XKP
RETURN
END
SUBROUTINE CALSIN(X,AMINUS)
XCOV=1.E-50
A1=1.-X
IF(A1) 4,6,9
9 X=1
AMINUS=0
4 FACT=1
TEMP=((-1.)**(K+1))*X**(2.*K)

```